MULTIMESSENGER STUDIES WITH THE PIERRE AUGER OBSERVATORY

Jon Paul Lundquist
jplundquist@gmail.com

University of Nova Gorica
www.ung.si/en/research/cac/

PIERRE AUGER OBSERVATORY

XIII International Conference on New Frontiers in Physics
26 Aug - 4 Sep 2024, OAC, Kolymbari, Crete, Greece

ABSTRACT SUMMARY


CHAT-GPT

- Pierre Auger Observatory (Auger): world's largest ultra-high-energy cosmic ray (UHECR) detector.
- Crucial role in multi-messenger astroparticle physics: high sensitivity to UHE photons and neutrinos.
- Set stringent limits on diffuse/point-like fluxes: constraints on dark-matter models and UHECR sources.
- No temporal coincidences of neutrinos/photons with LIGO/Virgo gravitational waves: energy flux limits.
- Lack of correlations between UHECR and HE neutrinos from IceCube Neutrino Observatory, ANTARES, and Auger: additional flux constraints.
- No significant UHE neutron fluxes from galactic gamma-ray sources.

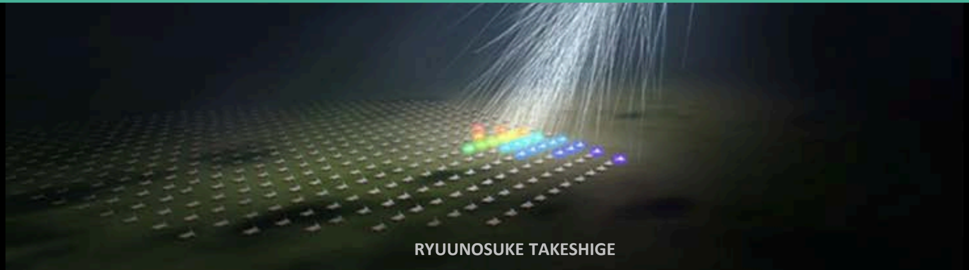
RYUUNOSUKE TAKESHIGE

ABSTRACT SUMMARY

- Pierre Auger Observatory (Auger): world's largest ultra-high-energy cosmic ray (UHECR) detector.
- Crucial role in multi-messenger astroparticle physics: high sensitivity to UHE photons and neutrinos.
- Set stringent limits on diffuse/point-like fluxes: constraints on dark-matter models and UHECR sources.
- No temporal coincidences of neutrinos/photons with LIGO/Virgo gravitational waves: energy flux limits.
- Lack of correlations between UHECR and HE neutrinos from IceCube Neutrino Observatory, ANTARES, and Auger: additional flux constraints.
- No significant UHE neutron fluxes from galactic gamma-ray sources.

See Tim Fehler's ICNFP2024 talk
"Searches for ultra-high-energy photons with the Pierre Auger Observatory: Current status and future perspectives"

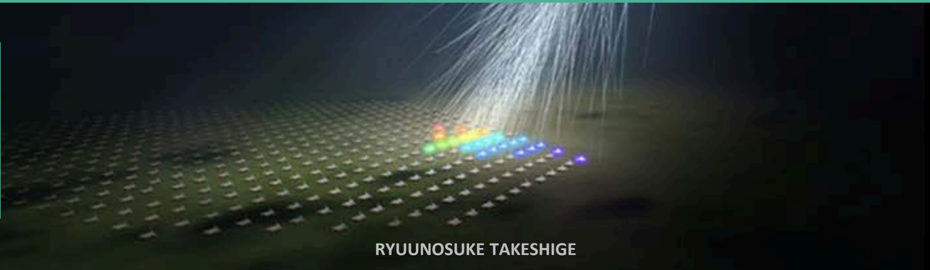

PIERRE AUGER OBSERVATORY

Highest energy multi-eye event

- **UHECR Hybrid Fluorescence and Ground Array Detector.**
- **E > 10^17 eV**
- **Located near Malargüe, Argentina**
- **>500 Worldwide Members**
- **First Results: 2004**

$3000\ \mathrm{km}^2$
18.5×Ljubljana

Ultra-High-Energy Cosmic Ray
Extensive Air-Shower
Particles

Five Fluorescence Detectors (FD)

~1600 Surface Detectors (SD)

See Vitor de Souza's ICNFP2024 talk
"Highlights from the Pierre Auger Observatory"

PIERRE AUGER OBSERVATORY

Highest energy multi-eye event

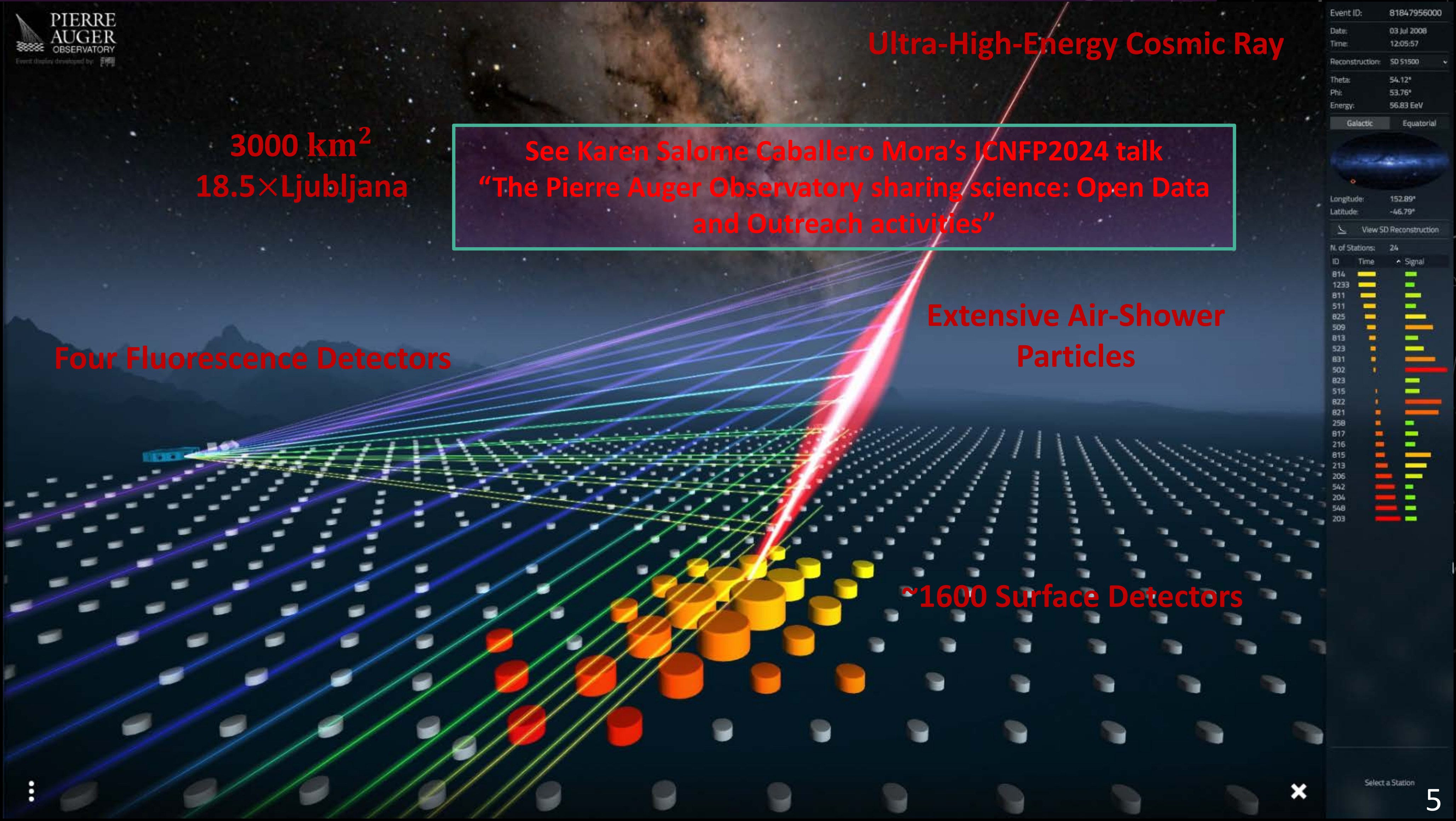

PIERRE AUGER OBSERVATORY
NEUTRINO DETECTION

AUGER NEUTRINOS

PoS (ICRC2023) 1488

- **UHE CRs and their sources produce neutrinos (cosmogenic and astrophysical).**
- **Neutral particles point back towards sources.**
- **Auger is sensitive to UHE neutrinos: $E_\nu > \sim 10^{17}$ eV.**

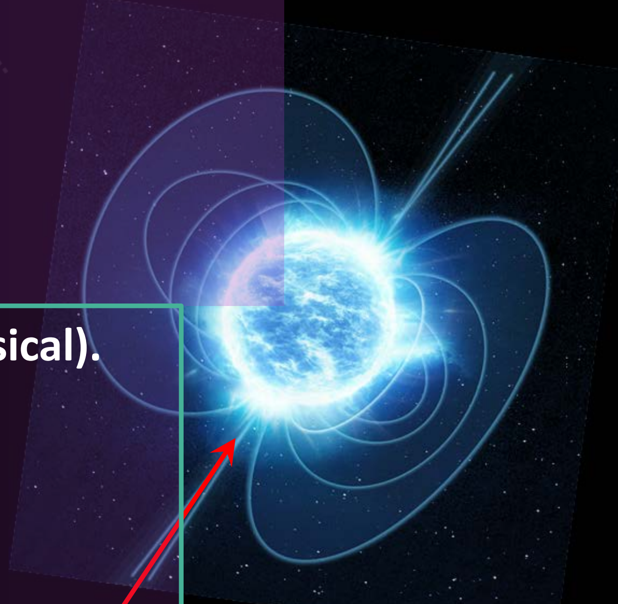

EUROPEAN SPACE AGENCY

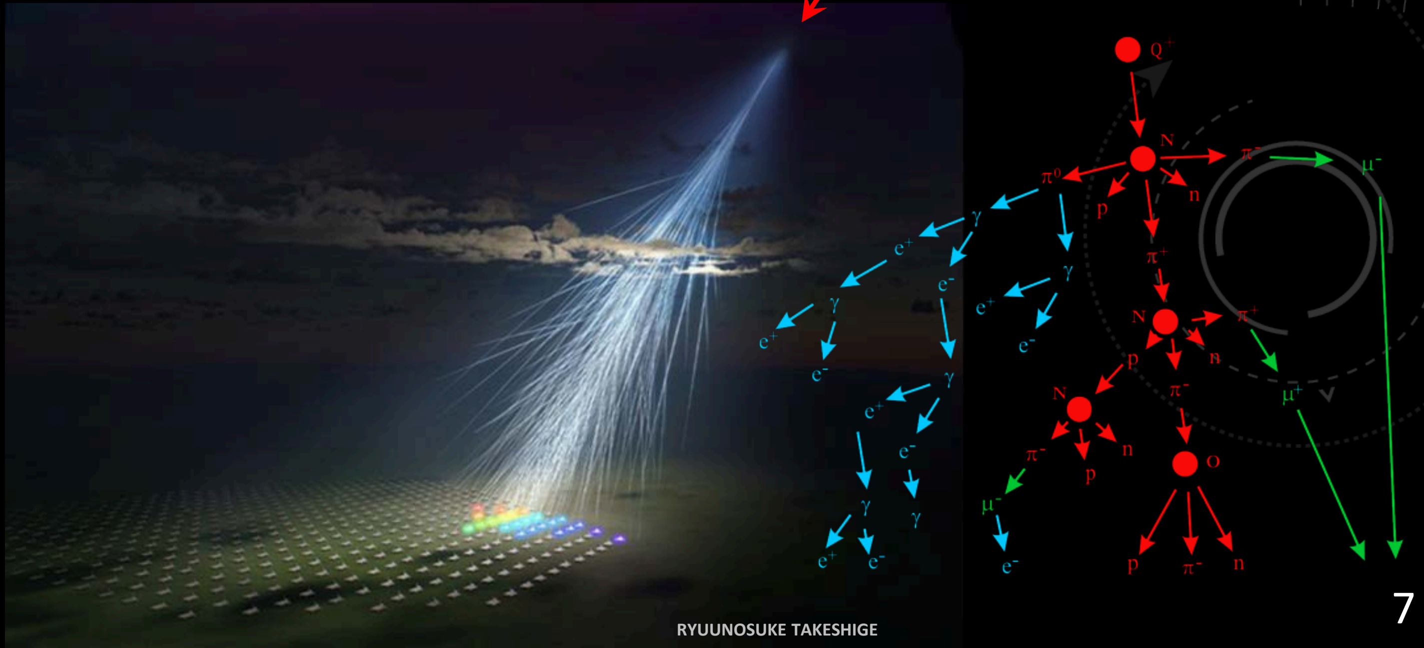

RYUUNOSUKE TAKESHIGE

AUGER NEUTRINOS

PoS (ICRC2023) 1488

- UHE CRs and their sources produce neutrinos (cosmogenic and astrophysical).
- Neutral particles point back towards sources.
- Auger is sensitive to UHE neutrinos: $E_\nu > \sim 10^{17}$ eV.

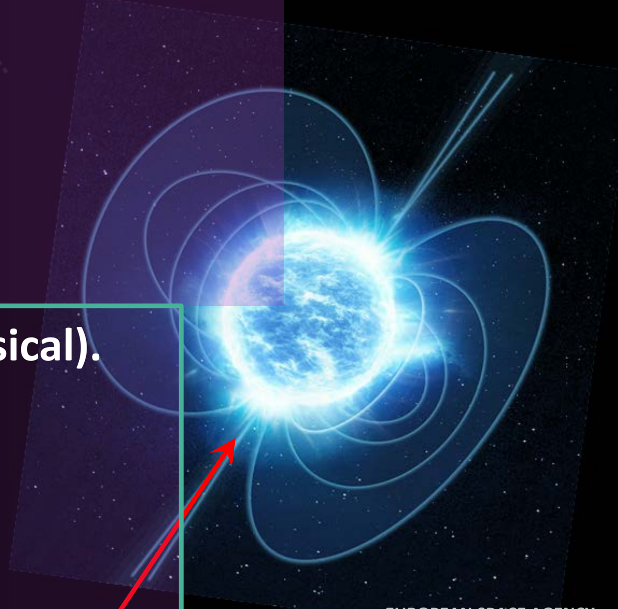

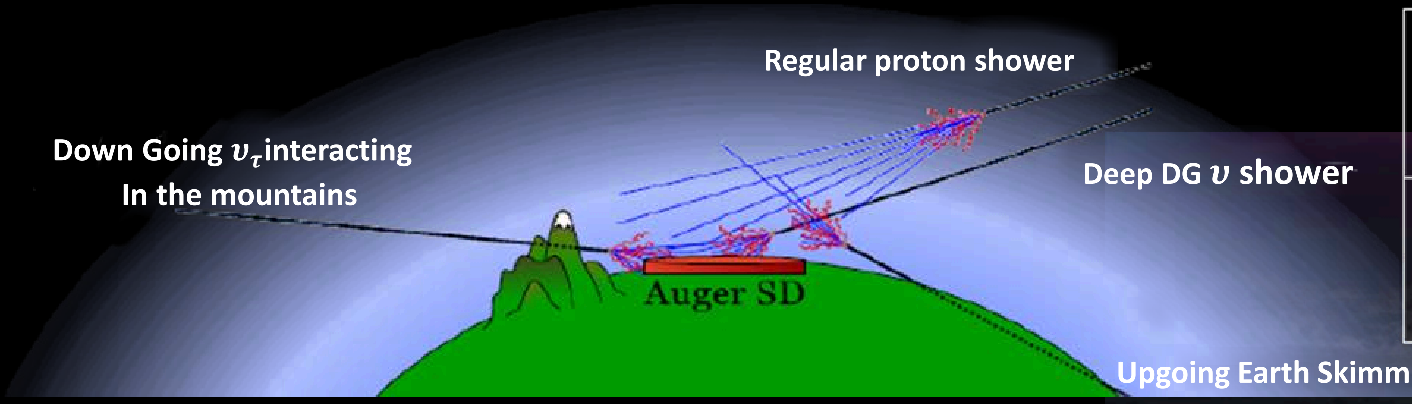

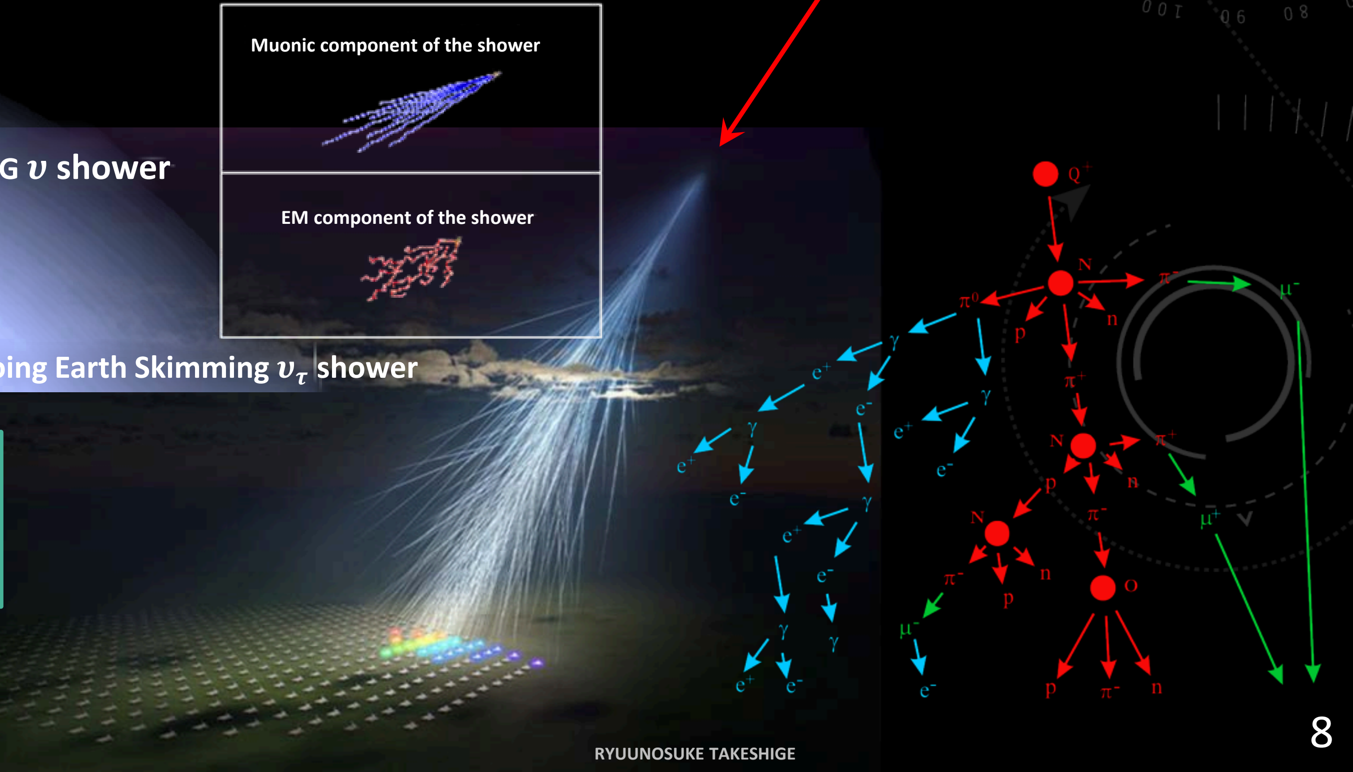

Deep Initiated Showers
- Weak Muonic Component
- Strong EM Component

SD NEUTRINO SEARCH

PoS (ICRC2023) 1488

- Hadronic showers start high in the atmosphere: EM is absorbed.
- Neutrinos: High-inclination showers with strong EM component.

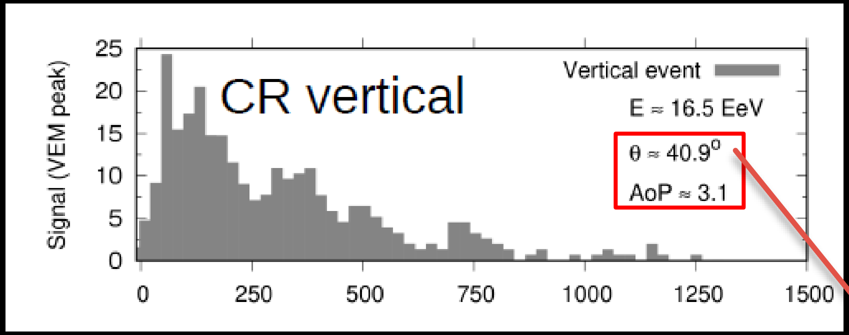

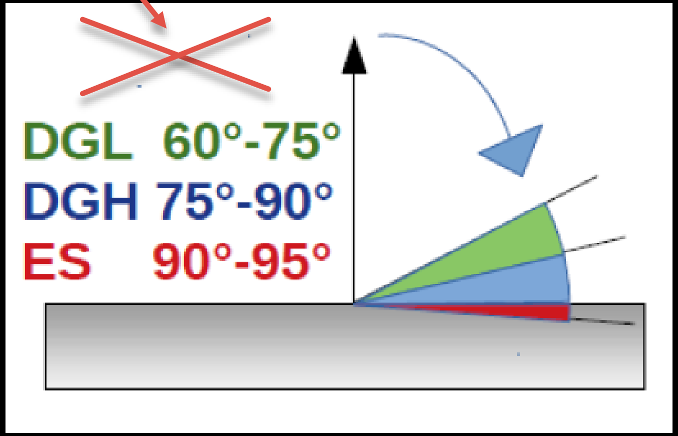

Example SD Signals

SD NEUTRINO SEARCH

PoS (ICRC2023) 1488

→ Inclined events with slow rising and broad signal
→ Larger Area-over-Peak (AoP)

- **Hadronic showers start high in the atmosphere: EM is absorbed.**
- **Neutrinos: High-inclination showers with strong EM component.**

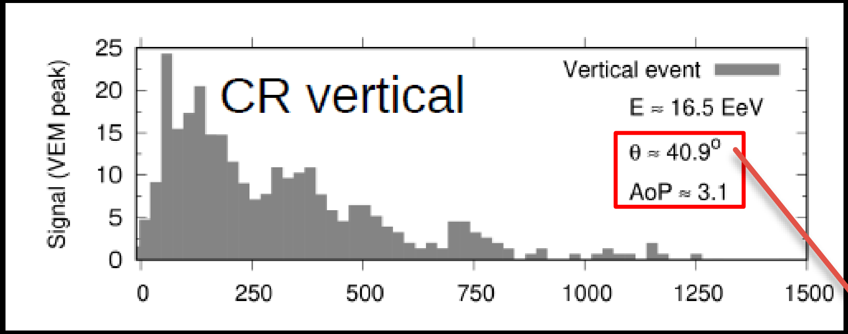

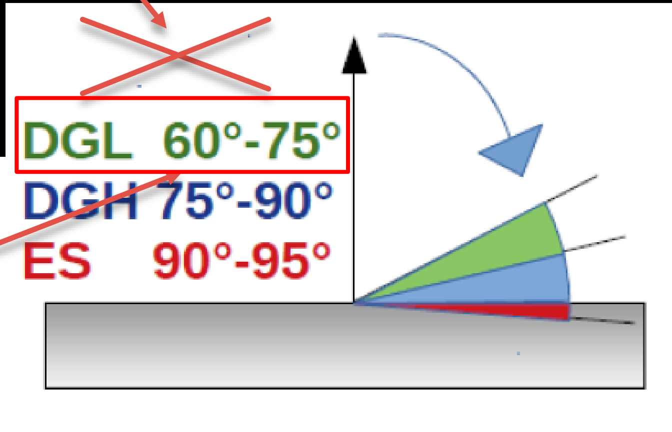

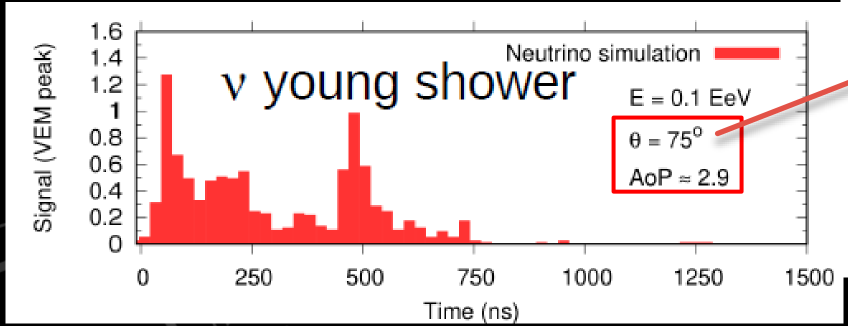

Example SD Signals

SD NEUTRINO SEARCH

PoS (ICRC2023) 1488

→ Inclined events with slow rising and broad signal
→ Larger Area-over-Peak (AoP)

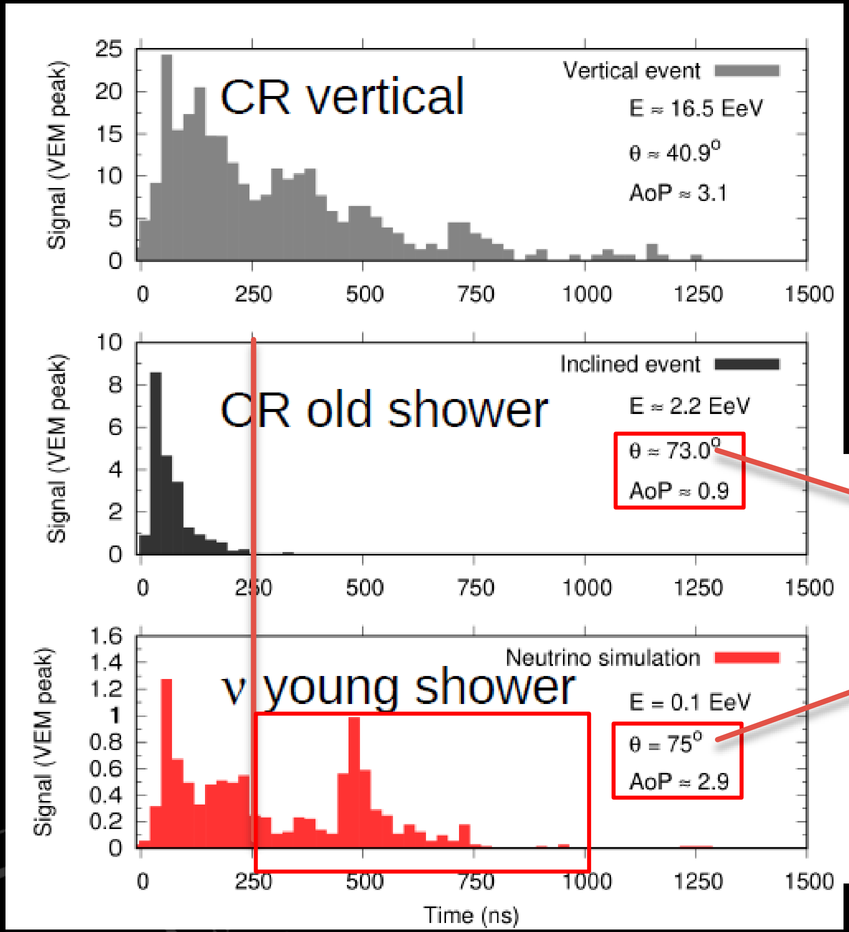

Example SD Signals

- Hadronic showers start high in the atmosphere: EM is absorbed.
- Neutrinos: High-inclination showers with strong EM component.
- Large surface detector signal time spread.
    - Large average SD signal area over peak $\langle AoP \rangle$.
- Upward going Earth-skimming events.

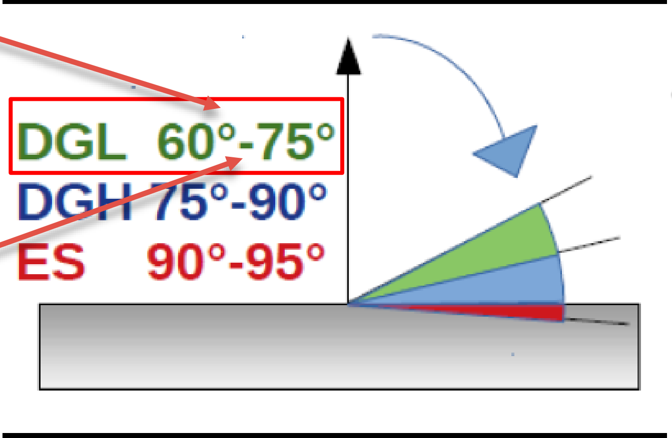

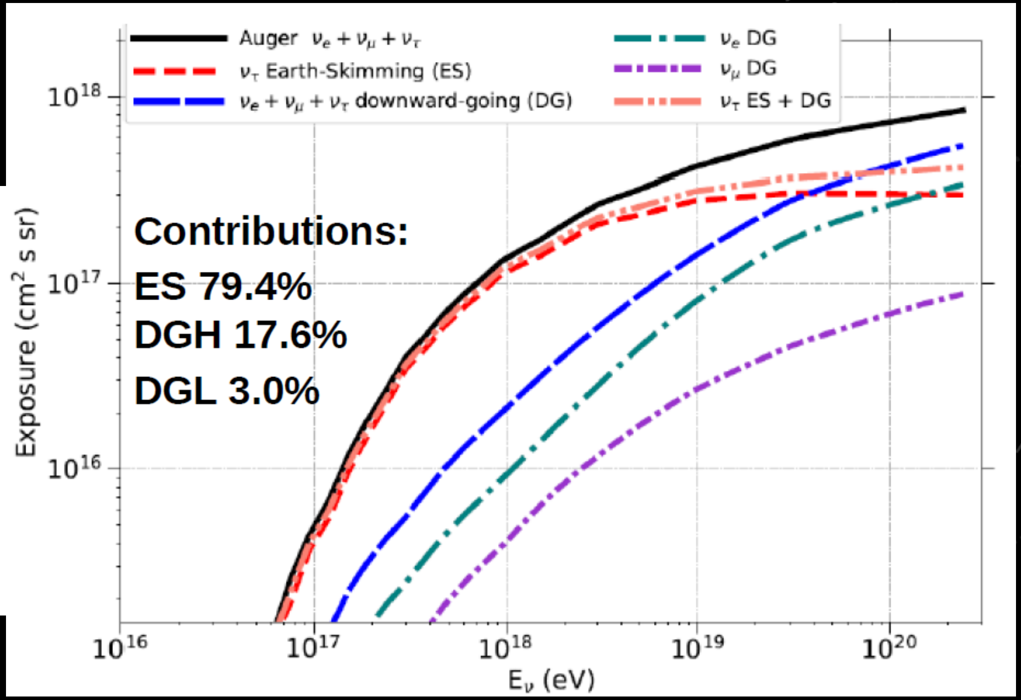

SD NEUTRINO SEARCH

PoS (ICRC2023) 1488

- Hadronic showers start high in the atmosphere: EM is absorbed.
- Neutrinos: High-inclination showers with strong EM component.
- Large surface detector signal time spread.
  - Large average SD signal area over peak $\langle AoP \rangle$.
- Upward going Earth-skimming events.

False-positives: 1/(50 years)

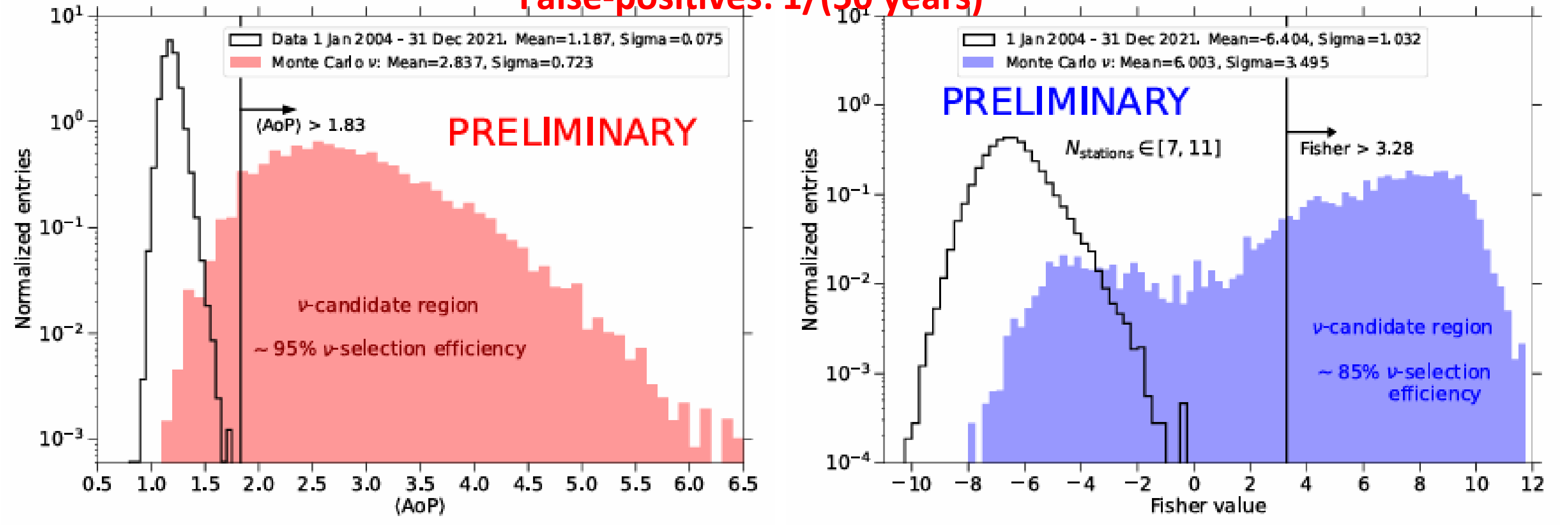

Earth-Skimming $\langle AoP \rangle$ Search

Down-going Fisher Discriminant MVA - $\langle AoP \rangle$ and time spread info

SD NEUTRINO SEARCH

PoS (ICRC2023) 1488

- **Competitive Upper-limits.**
  - $k \sim 3.5 \times 10^{-9}$ GeV cm^{-2} s^{-1} sr^{-1} (10^{17} *to* $10^{19.7}$ eV)
- **Pure-proton composition and a strong source redshift evolutions are excluded**

$$\frac{dN(E_v)}{dE_v} = k \cdot E_v^{-2}$$

EPJ 283 (2023) 04003.004

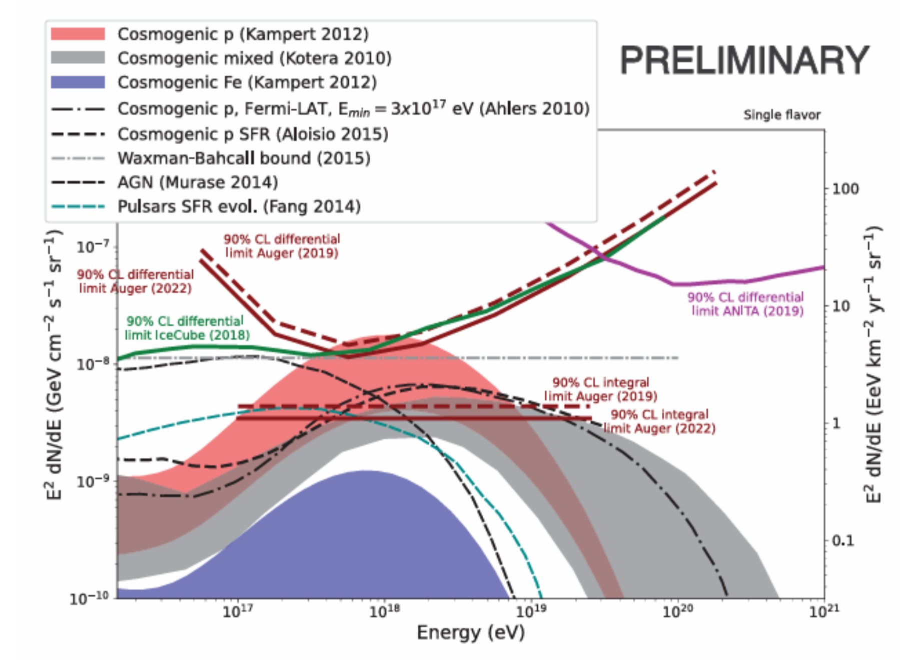

Diffuse Neutrino Upper Limits

JCAP 11 (2019) 004

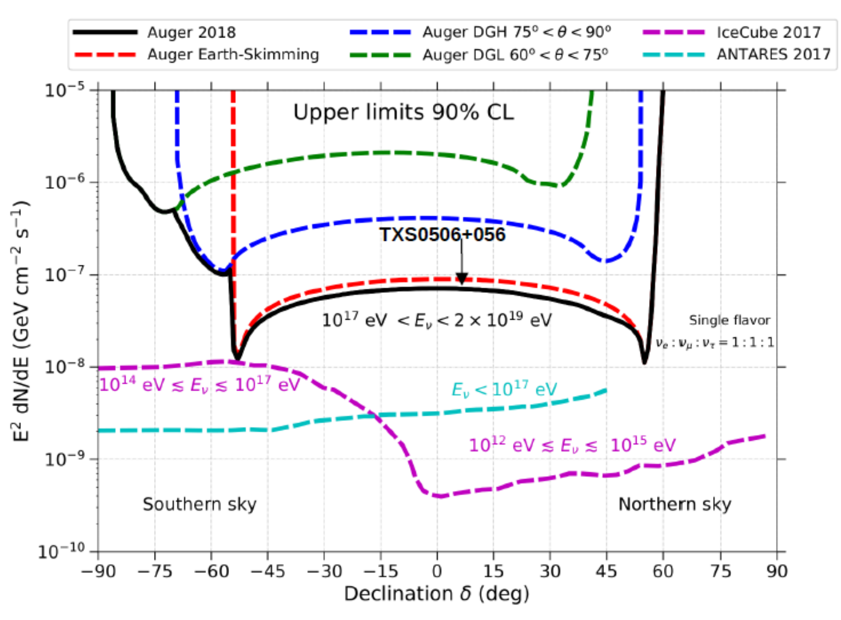

Declination Dependent "Point-Source" Upper Limits

SD NEUTRINO SEARCH

PoS (ICRC2023) 1488

- Competitive Upper-limits.
  - $k \sim 3.5 \times 10^{-9}$ GeV cm^{-2} s^{-1} sr^{-1} (10^{17} *to* $10^{19.7}$ eV)
- Pure-proton composition and a strong source redshift evolutions are excluded

$$\frac{dN(E_\nu)}{dE_\nu} = k \cdot E_\nu^{-2}$$

PoS (ICRC2023) 1520

EPJ 283 (2023) 04003.004

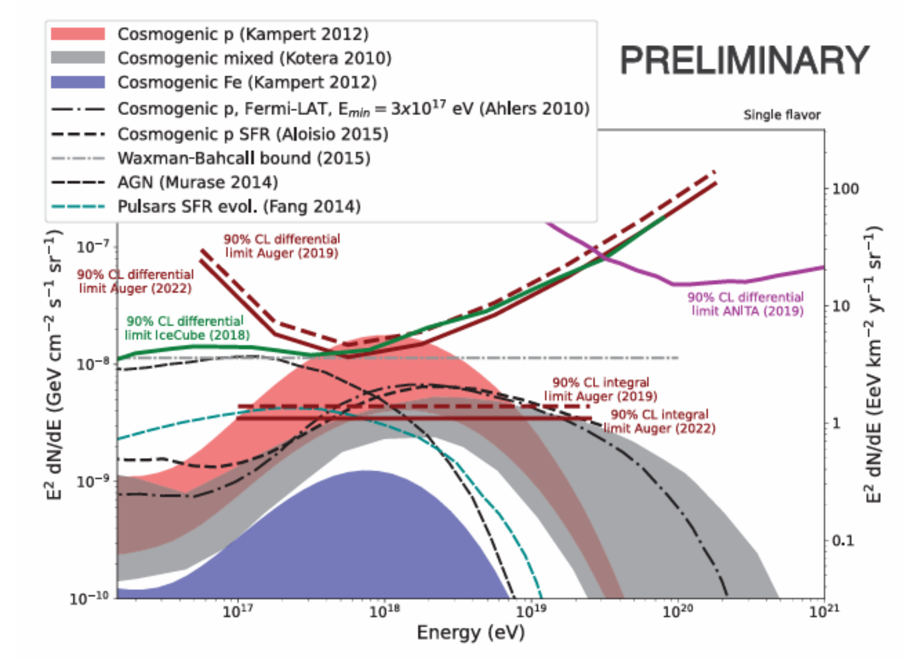

Diffuse Neutrino Upper Limits

JCAP 11 (2019) 004

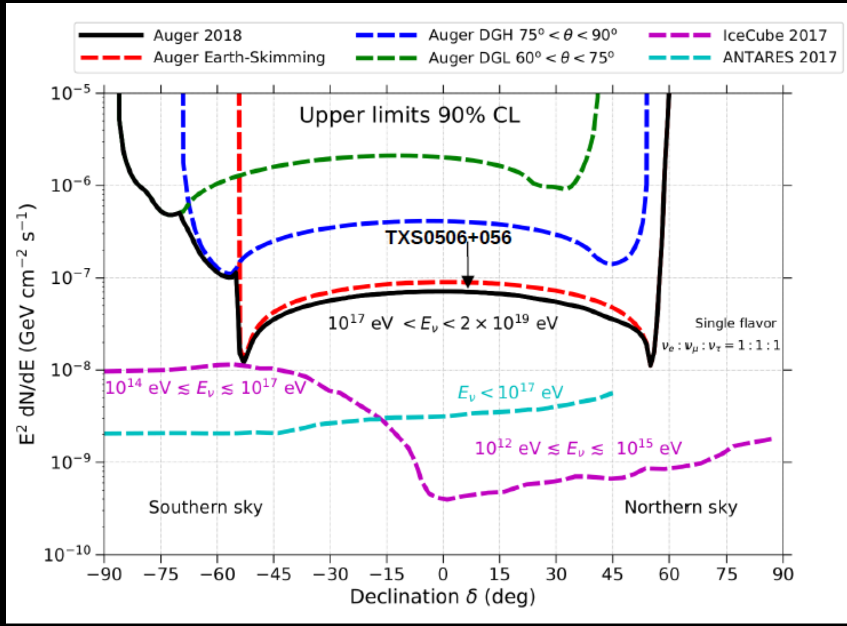

Declination Dependent "Point-Source" Upper Limits

AUGER NEUTRINOS AND GRAVITATIONAL WAVES

BINARY BLACK HOLE MERGER NEUTRINOS

PoS (ICRC2023) 1488

- UHE neutrino luminosity of binary black hole mergers observed by the LIGO/Virgo Collaboration (LVC) via stacking analysis (2015-2020).

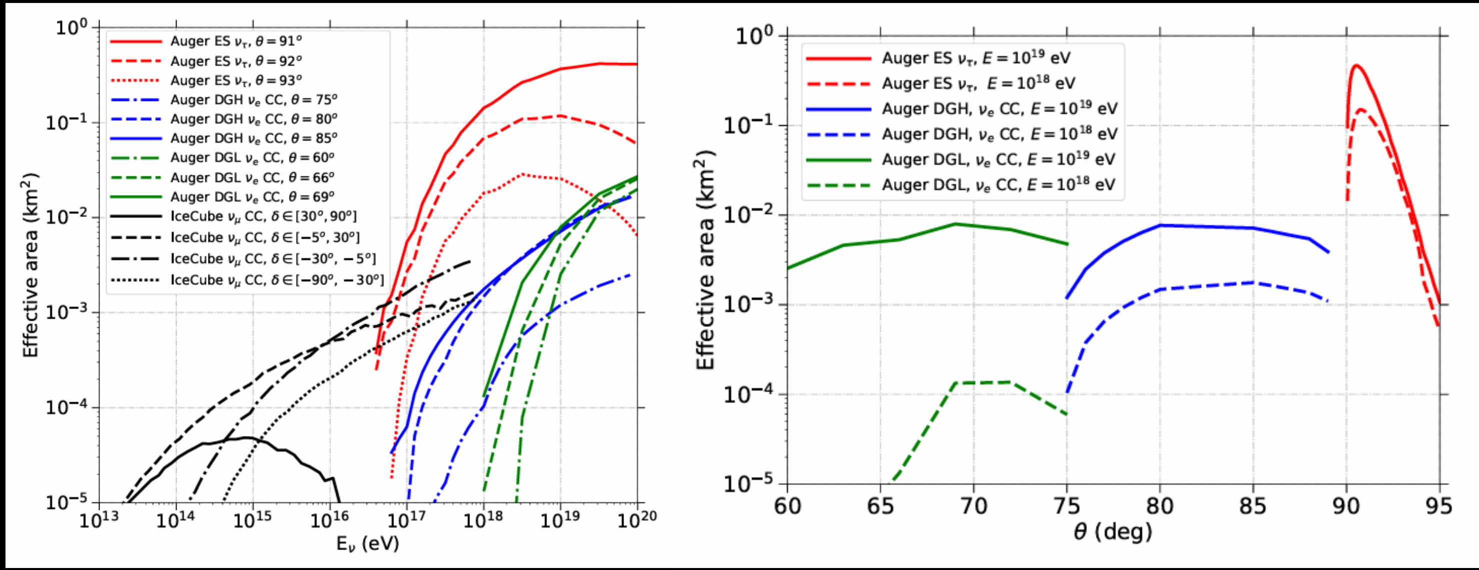

- Effective Detector Area dependence:
  - Zenith Angle θ ("channel")
  - Neutrino Energy E_ν
  - Time
    - Short-term SD Behavior
    - Pointing-direction's Zenith Angle $\theta(t)$

JCAP 11, 004 (2019)

BINARY BLACK HOLE MERGER NEUTRINOS

PoS (ICRC2023) 1488

- **UHE neutrino luminosity of binary black hole mergers observed by the LIGO/Virgo Collaboration (LVC) via stacking analysis (2015-2020).**

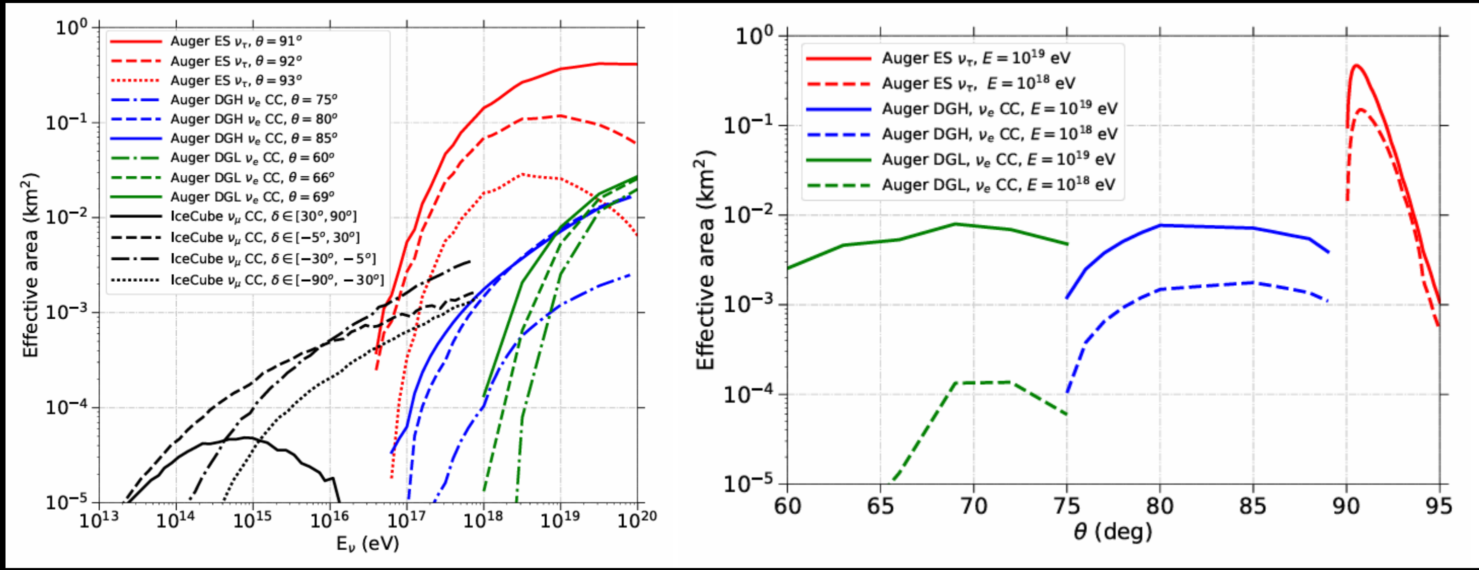

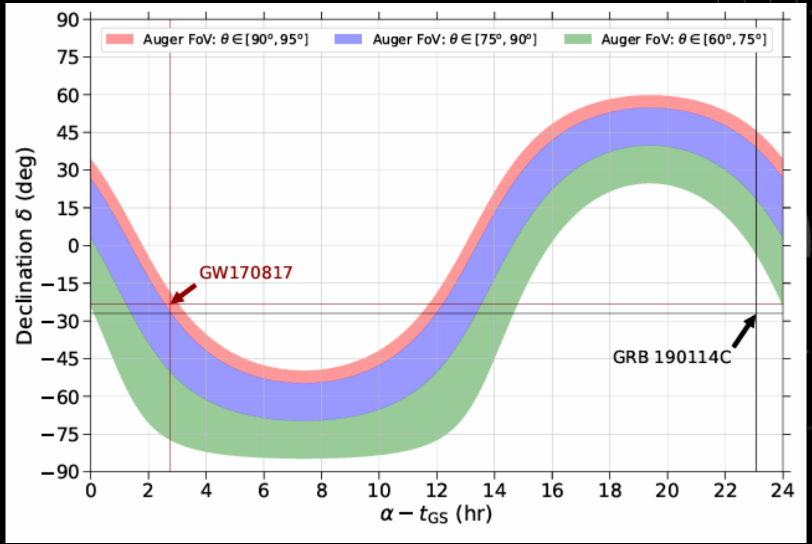

- **Effective Detector Area dependence:**
  - Zenith Angle θ ("channel")
  - Neutrino Energy E_ν
  - Time
    - Short-term SD Behavior
    - Pointing-direction's Zenith Angle $\theta(t)$

JCAP 11, 004 (2019)

BINARY BLACK HOLE MERGER NEUTRINOS

PoS (ICRC2023) 1488

- UHE neutrino luminosity of binary black hole mergers observed by the LIGO/Virgo Collaboration (LVC) via stacking analysis (2015-2020).

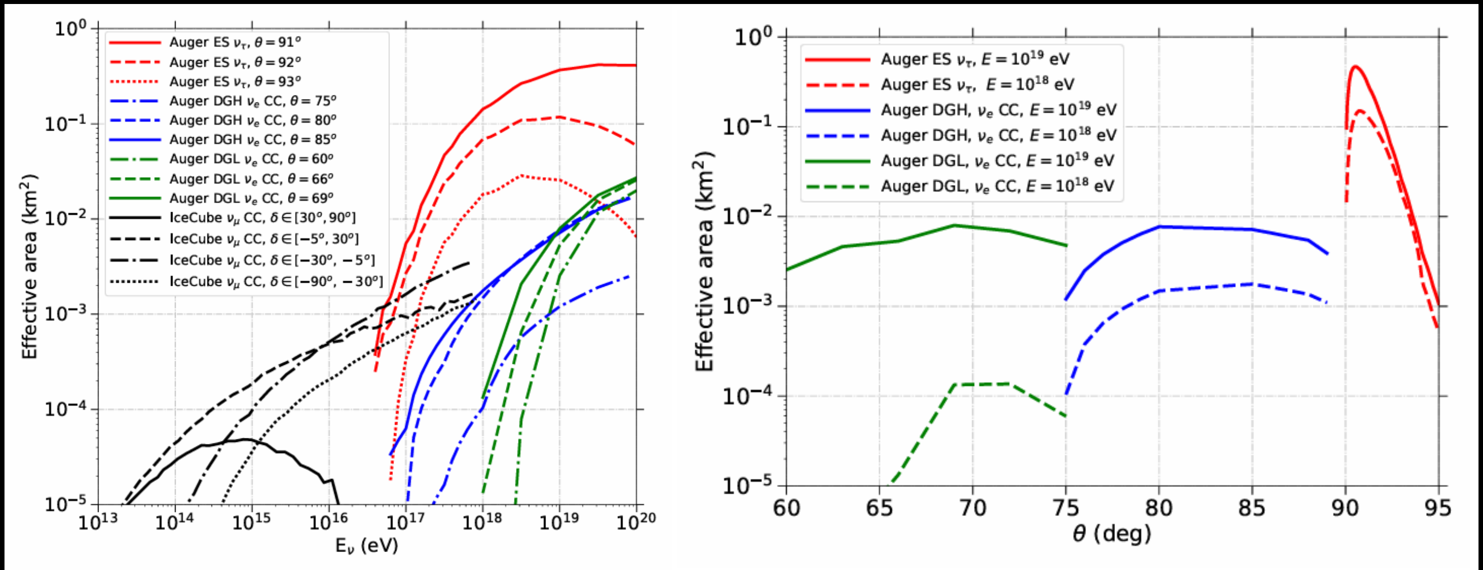

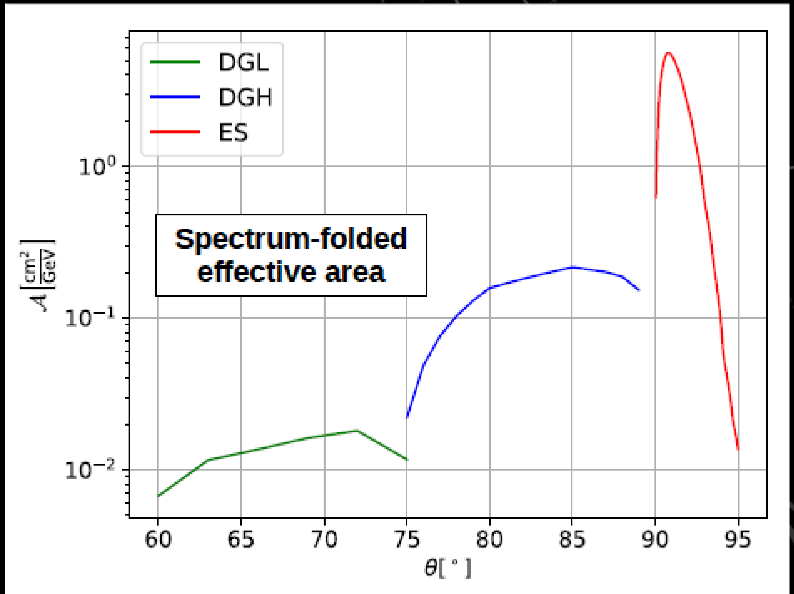

- Effective Detector Area dependence:
  - Zenith Angle θ ("channel")
  - Neutrino Energy E_ν
  - Time
    - Short-term SD Behavior
    - Pointing-direction's Zenith Angle $\theta(t)$

$$\mathcal{A}(\theta, t) = \int_0^\infty E_\nu^{-2} \; A_{eff}(E_\nu, \theta(t), t) \; dE_\nu$$

- Assumed Neutrino Spectrum

JCAP 11, 004 (2019)

BINARY BLACK HOLE MERGER NEUTRINOS

PoS (ICRC2023) 1488

- UHE neutrino luminosity of binary black hole mergers observed by the LIGO/Virgo Collaboration (LVC) via stacking analysis (2015-2020).
- Isotropic E_ν^{-2} emission assumed.

$$L_{up,i} = \frac{N_{up,\nu}}{T_i}\left(\sum_{s}\sum_{p\epsilon\Omega_{90}(s)} A_{p,s,i}P_{p,s}\int_0^\infty \frac{\Pi_{p,s}(r)}{r^2(1+z(r))}dr\right)^{-1}$$

$L_{up,i}$ 90% CL Upper-Limit Neutrino Luminosity

- i: Time Bin, s: BBH Mergers, p: Healpix pixel locations.

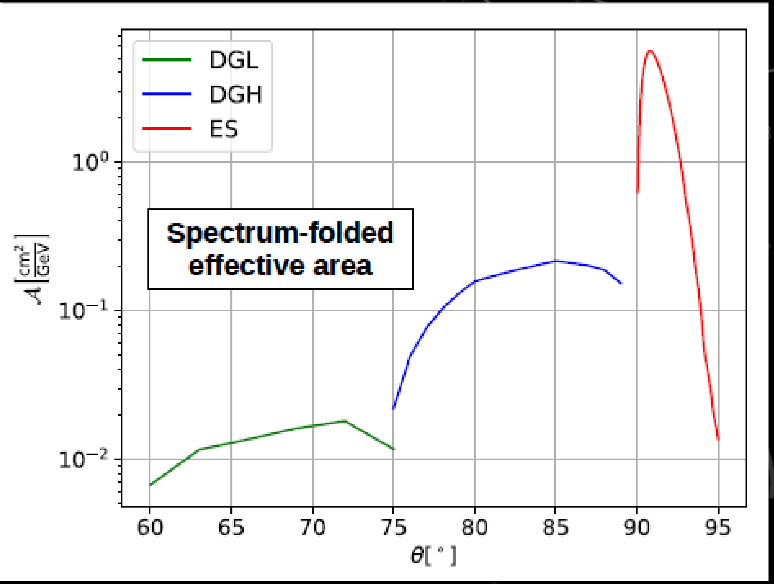

$$A(\theta,t) = \int_0^\infty E_\nu^{-2}\ A_{eff}(E_\nu,\theta(t),t)\ dE_\nu$$

JCAP 11, 004 (2019)

BINARY BLACK HOLE MERGER NEUTRINOS

PoS (ICRC2023) 1488

- UHE neutrino luminosity of binary black hole mergers observed by the LIGO/Virgo Collaboration (LVC) via stacking analysis (2015-2020).
- Isotropic E_ν^{-2} emission assumed.

$$L_{up,i} = \frac{N_{up,\nu}}{T_i}\left(\sum_{s}\sum_{p\epsilon\Omega_{90}(s)} A_{p,s,i}P_{p,s}\int_0^\infty \frac{\Pi_{p,s}(r)}{r^2\left(1+z(r)\right)}dr\right)^{-1}$$

$L_{up,i}$ 90% CL Upper-Limit Neutrino Luminosity

- i: Time Bin, s: BBH Mergers, p: Healpix pixel locations.

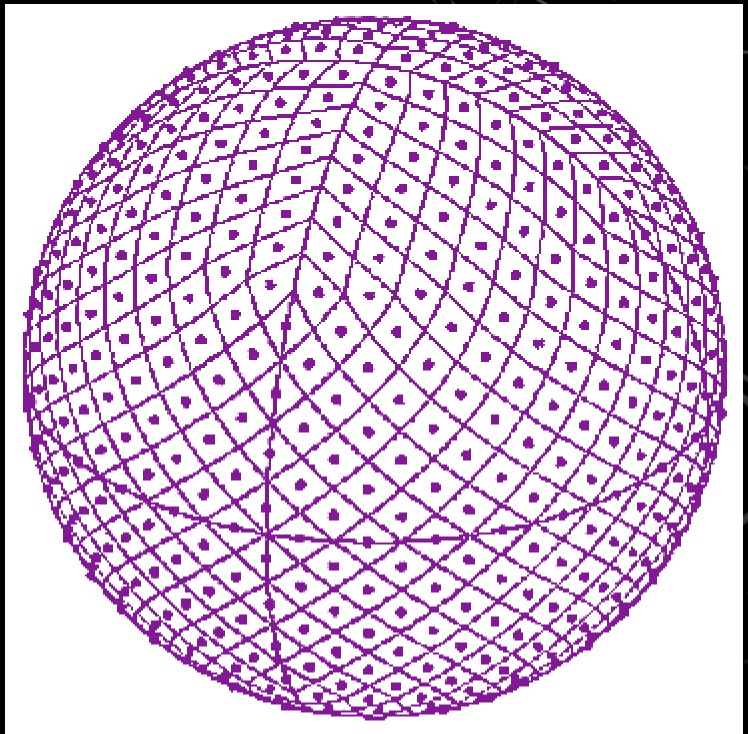

BINARY BLACK HOLE MERGER NEUTRINOS

PoS (ICRC2023) 1488

- UHE neutrino luminosity of binary black hole mergers observed by the LIGO/Virgo Collaboration (LVC) via stacking analysis (2015-2020).
- Isotropic E_ν^{-2} emission assumed.

$$L_{up,i} = \frac{N_{up,\nu}}{T_i}\left(\sum_{s}\sum_{p\epsilon\Omega_{90}(s)} A_{p,s,i} P_{p,s}\int_0^\infty \frac{\Pi_{p,s}(r)}{r^2(1+z(r))}dr\right)^{-1}$$

$L_{up,i}$ 90% CL Upper-Limit Neutrino Luminosity

- i: Time Bin, s: BBH Mergers, p: Healpix pixel locations.

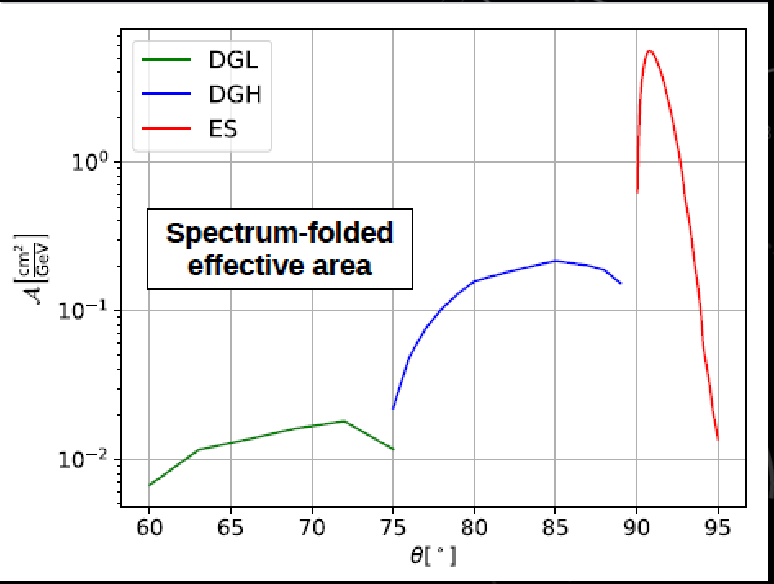

$$A(\theta,t) = \int_0^\infty E_\nu^{-2}\ A_{eff}(E_\nu,\theta(t),t)\ dE_\nu$$

JCAP 11, 004 (2019)

BINARY BLACK HOLE MERGER NEUTRINOS

PoS (ICRC2023) 1488

- UHE neutrino luminosity of binary black hole mergers observed by the LIGO/Virgo Collaboration (LVC) via stacking analysis (2015-2020).
- Isotropic E_ν^{-2} emission assumed.

$$L_{up,i} = \frac{N_{up,\nu}}{T_i} \left(\sum_{s} \sum_{p \epsilon \Omega_{90}(s)} A_{p,s,i} P_{p,s} \int_0^\infty \frac{\Pi_{p,s}(r)}{r^2 (1 + z(r))} dr \right)^{-1}$$

$L_{up,i}$ 90% CL Upper-Limit Neutrino Luminosity

- i: Time Bin, s: BBH Mergers, p: Healpix pixel locations.
- $N_{up,\nu} = 2.44$: Non-observation 90% CL.

BINARY BLACK HOLE MERGER NEUTRINOS

PoS (ICRC2023) 1488

- **UHE neutrino luminosity of binary black hole mergers observed by the LIGO/Virgo Collaboration (LVC) via stacking analysis (2015-2020).**
- **Isotropic E_ν^{-2} emission assumed.**

$$L_{up,i} = \frac{N_{up,\nu}}{T_i}\left(\sum_{s}\sum_{p\epsilon\Omega_{90}(s)} A_{p,s,i}P_{p,s}\int_0^\infty \frac{\Pi_{p,s}(r)}{r^2(1+z(r))}dr\right)^{-1}$$

$L_{up,i}$ 90% CL Upper-Limit Neutrino Luminosity

- **i: Time Bin, s: BBH Mergers, p: Healpix pixel locations.**
- **$N_{up,\nu} = 2.44$: Non-observation 90% CL.**
- **$p\epsilon\Omega_{90}(s)$: Pixels inside 90% CL Solid Angle of Source.**

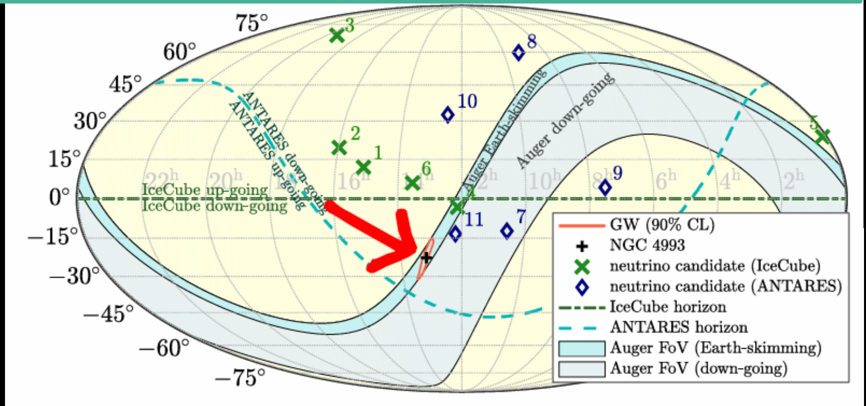

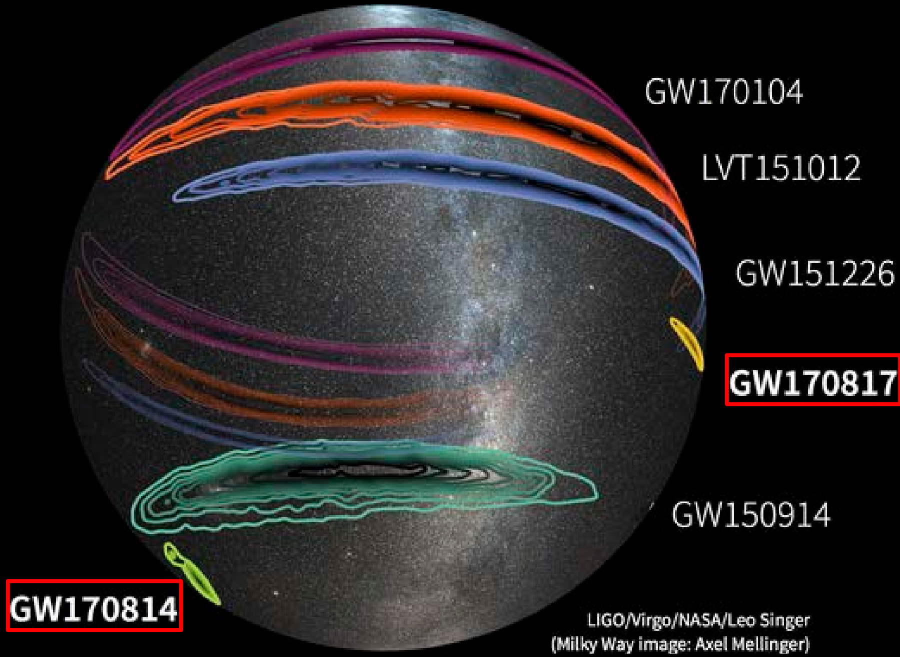

BINARY BLACK HOLE MERGER NEUTRINOS

PoS (ICRC2023) 1488

- UHE neutrino luminosity of binary black hole mergers observed by the LIGO/Virgo Collaboration (LVC) via stacking analysis (2015-2020).
- Isotropic E_ν^{-2} emission assumed.

$$L_{up,i} = \frac{N_{up,\nu}}{T_i}\left(\sum_{s}\sum_{p\epsilon\Omega_{90}(s)} A_{p,s,i} P_{p,s} \int_0^\infty \frac{\Pi_{p,s}(r)}{r^2(1+z(r))}dr\right)^{-1}$$

$L_{up,i}$ 90% CL Upper-Limit Neutrino Luminosity

- i: Time Bin, s: BBH Mergers, p: Healpix pixel locations.
- $N_{up,\nu} = 2.44$: Non-observation 90% CL.
- $p\epsilon\Omega_{90}(s)$: Pixels inside 90% CL Solid Angle of Source.
- $P_{p,s}$: Source Probability (PDF) at Pointing Direction.

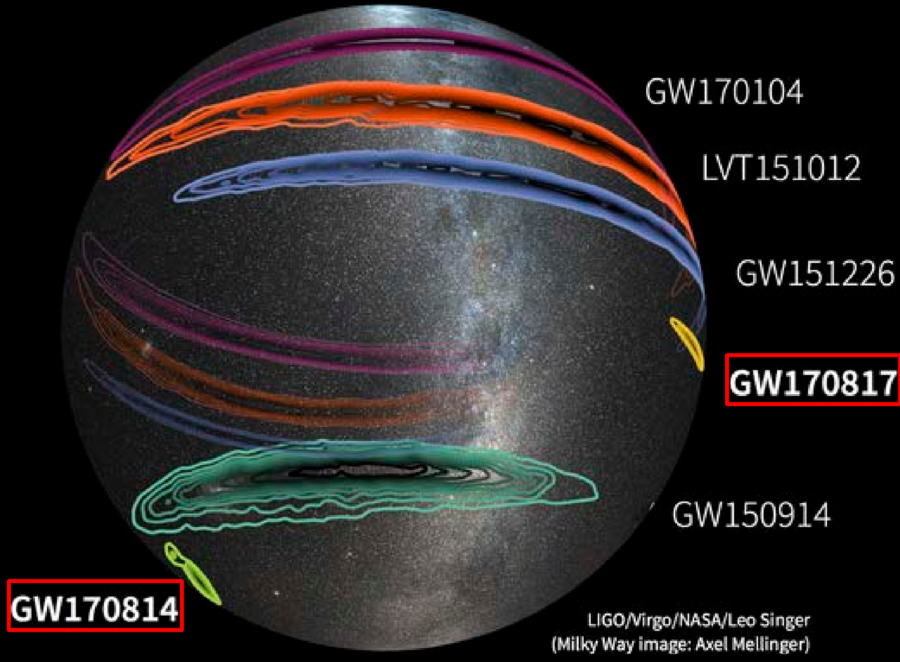

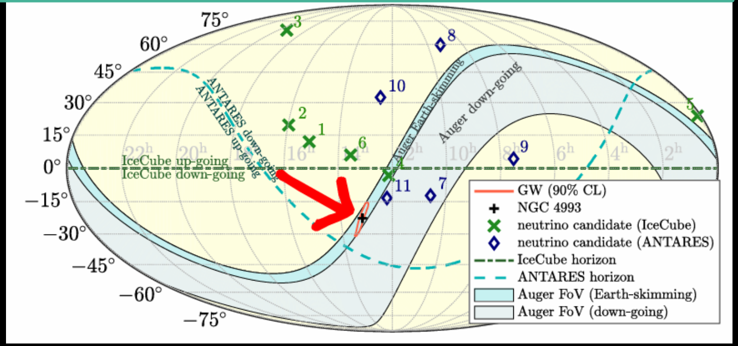

BINARY BLACK HOLE MERGER NEUTRINOS

PoS (ICRC2023) 1488

- UHE neutrino luminosity of binary black hole mergers observed by the LIGO/Virgo Collaboration (LVC) via stacking analysis (2015-2020).
- Isotropic E_ν^{-2} emission assumed.

$$L_{up,i} = \frac{N_{up,\nu}}{T_i}\left(\sum_{s}\sum_{p\epsilon\Omega_{90}(s)} A_{p,s,i}P_{p,s}\int_0^\infty \frac{\Pi_{p,s}(r)}{r^2(1+z(r))}dr\right)^{-1}$$

$L_{up,i}$ 90% CL Upper-Limit Neutrino Luminosity

- i: Time Bin, s: BBH Mergers, p: Healpix pixel locations.
- $N_{up,\nu} = 2.44$: Non-observation 90% CL.
- $p\epsilon\Omega_{90}(s)$: Pixels inside 90% CL Solid Angle of Source.
- $P_{p,s}$: Source Probability (PDF) at Pointing Direction.
- $\Pi_{p,s}(r)$: Luminosity Distance PDF.

$P_{p,s} * \Pi_{p,s}$ (3D info.)

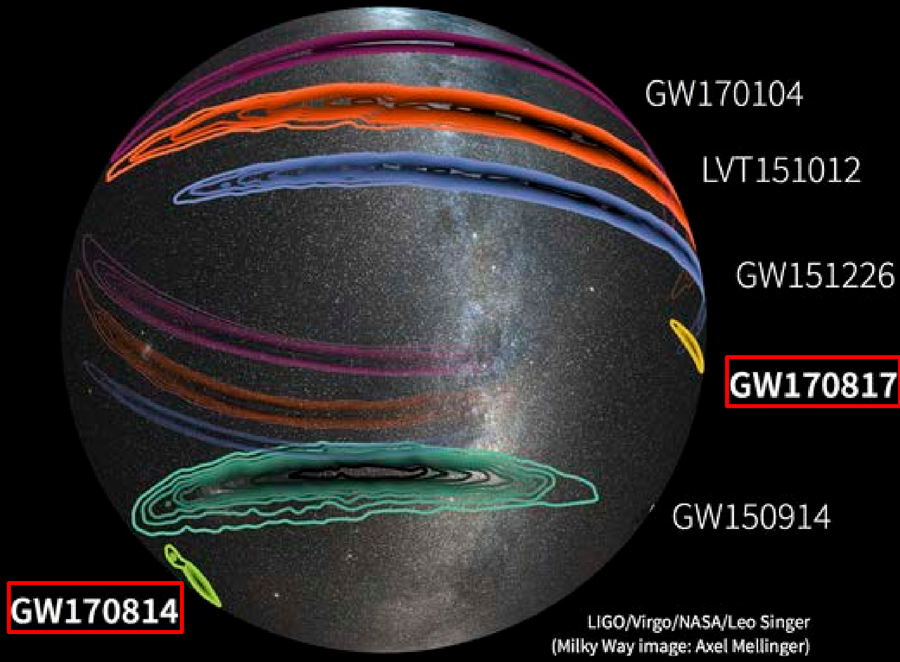

BINARY BLACK HOLE MERGER NEUTRINOS

PoS (ICRC2023) 1488

- UHE neutrino luminosity of binary black hole mergers observed by the LIGO/Virgo Collaboration (LVC) via stacking analysis (2015-2020).
- Isotropic E_ν^{-2} emission assumed.

$$L_{up,i} = \frac{N_{up,\nu}}{T_i}\left(\sum_{s}\sum_{p\epsilon\Omega_{90}(s)} A_{p,s,i}P_{p,s}\int_0^\infty \frac{\Pi_{p,s}(r)}{r^2(1+z(r))}dr\right)^{-1}$$

$L_{up,i}$ 90% CL Upper-Limit Neutrino Luminosity

- i: Time Bin, s: BBH Mergers, p: Healpix pixel locations.
- $N_{up,\nu} = 2.44$: Non-observation 90% CL.
- $p\epsilon\Omega_{90}(s)$: Pixels inside 90% CL Solid Angle of Source.
- $P_{p,s}$: Source Probability (PDF) at Pointing Direction.
- $\Pi_{p,s}(r)$: Luminosity Distance PDF.

$P_{p,s} * \Pi_{p,s}$ (3D info.)

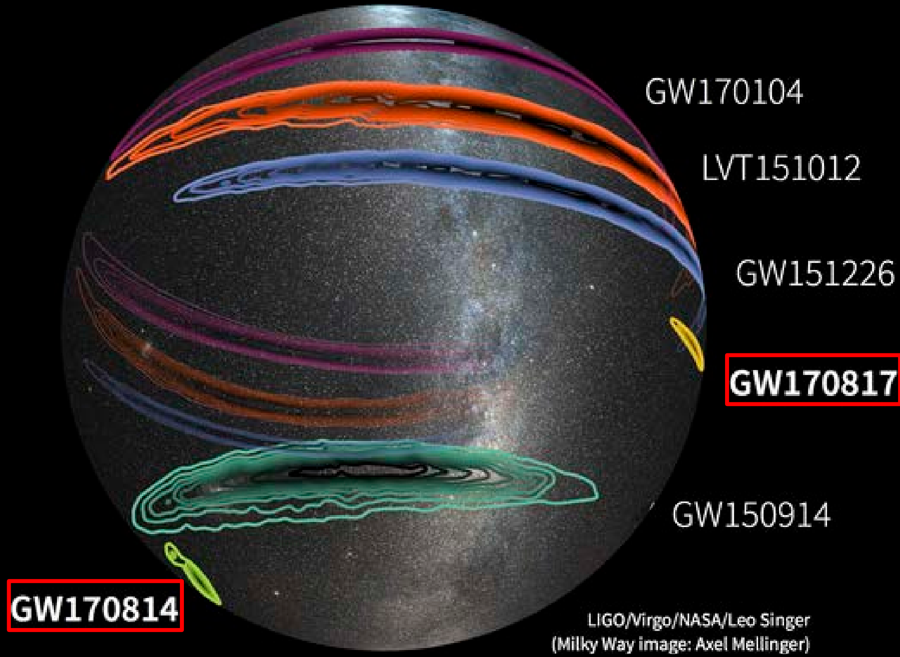

BINARY BLACK HOLE MERGER NEUTRINOS

PoS (ICRC2023) 1488

- UHE neutrino luminosity of BBH mergers observed by LVC via stacking analysis.
- Assuming constant luminosity Isotropic E_ν^{-2} spectrum during emission periods of 24 hours and 60 days after merger.

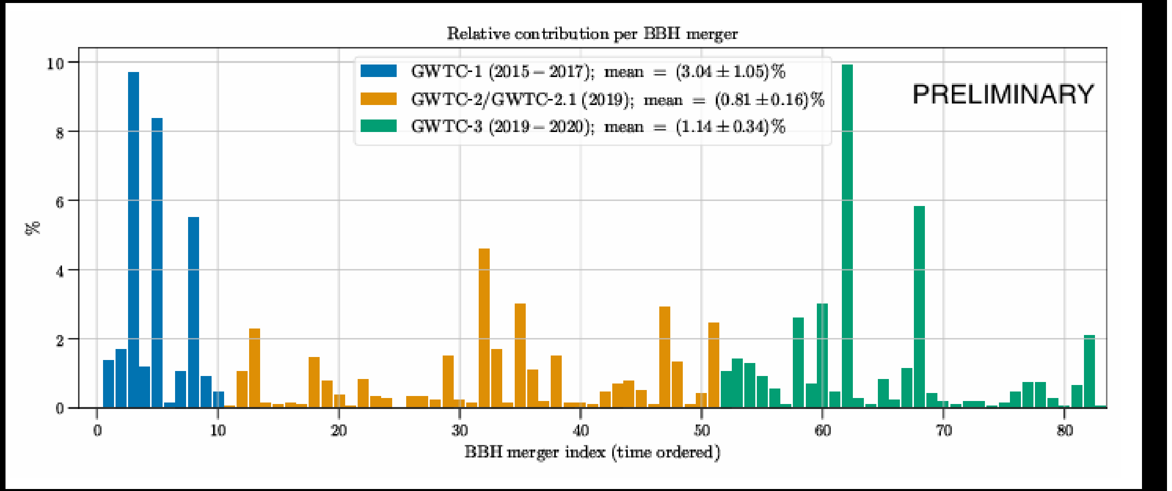

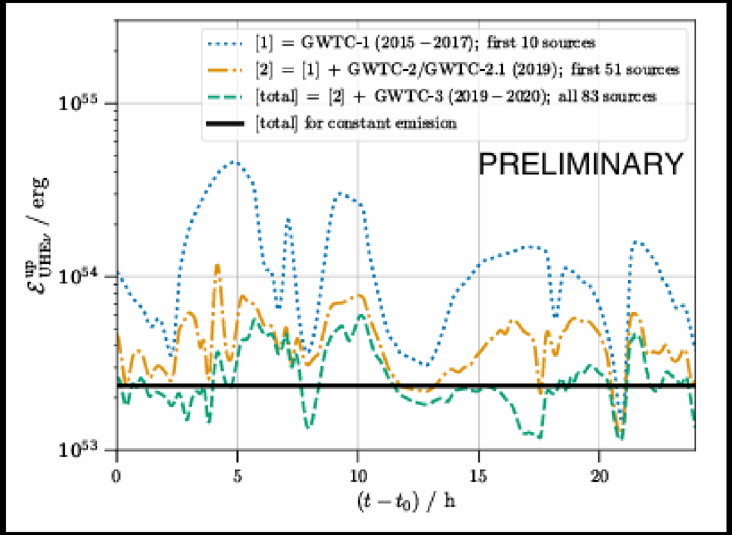

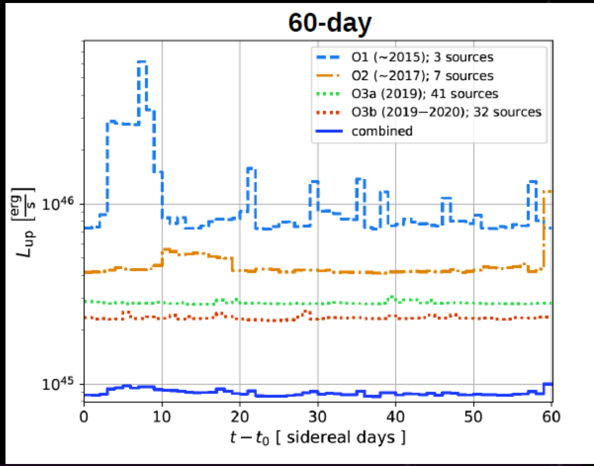

60 Day Period (older figure)

EPJ (UHECR2022) 283

- $L_{up,1day} = 2.7 \times 10^{48}$ erg/s
- $L_{up,60days} = 4.6 \times 10^{46}$ erg/s $\approx L_{up,1day}/60$

- $E_{up,1day} = 2.3 \times 10^{53}$ erg
- $E_{up,60days} = 2.4 \times 10^{53}$ erg

Stringent Upper Limits on UHE Neutrinos

BINARY BLACK HOLE MERGER NEUTRINOS

PoS (ICRC2023) 1488

- **UHE neutrino luminosity of BBH mergers observed by LVC via stacking analysis.**
- **Assuming constant luminosity Isotropic E_ν^{-2} spectrum during emission periods of 24 hours and 60 days after merger.**

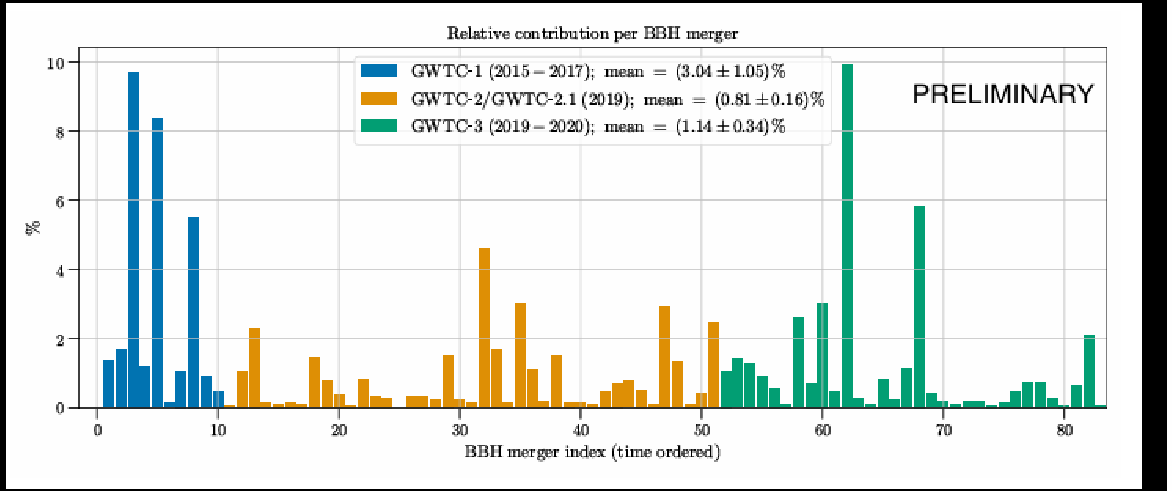

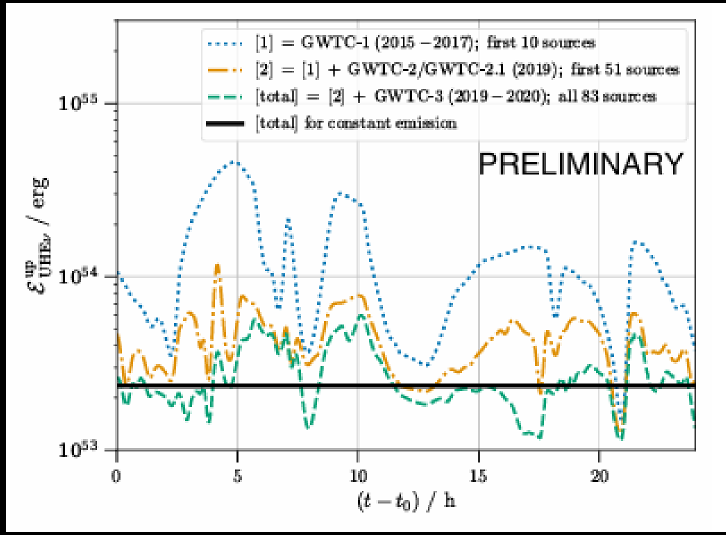

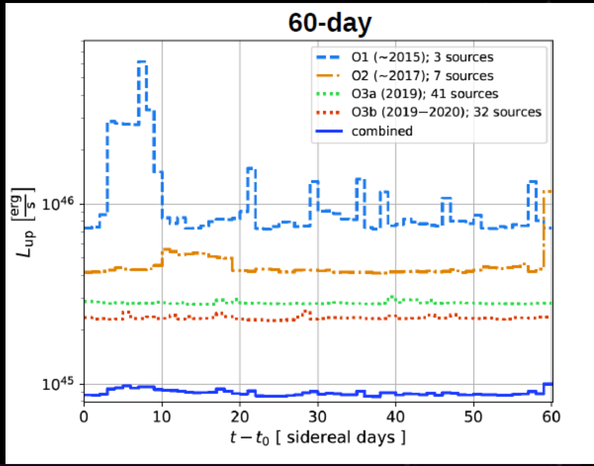

60 Day Period (older figure)

EPJ (UHECR2022) 283

UHE Neutrino U.L.: $\sim M_\odot c^2/10$

BBH Merger output: $\sim 2M_\odot c^2$

- $L_{up,1day} = 2.7 \times 10^{48}$ erg/s
- $L_{up,60days} = 4.6 \times 10^{46}$ erg/s $\approx L_{up,1day}/60$

- $E_{up,1day} = 2.3 \times 10^{53}$ erg
- $E_{up,60days} = 2.4 \times 10^{53}$ erg

Stringent Upper Limits on UHE Neutrinos

GW170817 (BINARY NEUTRON STAR MERGER)

ApJ Lett. 850 (2017)

- GW170817: Seen by 70 observatories (7 continents and space) across the EM spectrum
- Follow-up of gravitational-wave (GW) event alerts through, e.g., GCN
- SD neutrino search with <15 minute latency: both Earth-skimming (ES) and down-going (DG) channels – no neutrinos identified.
- Perfectly within the ES channel FoV at event time.
- Auger limits complement those of IceCube and ANTARES.

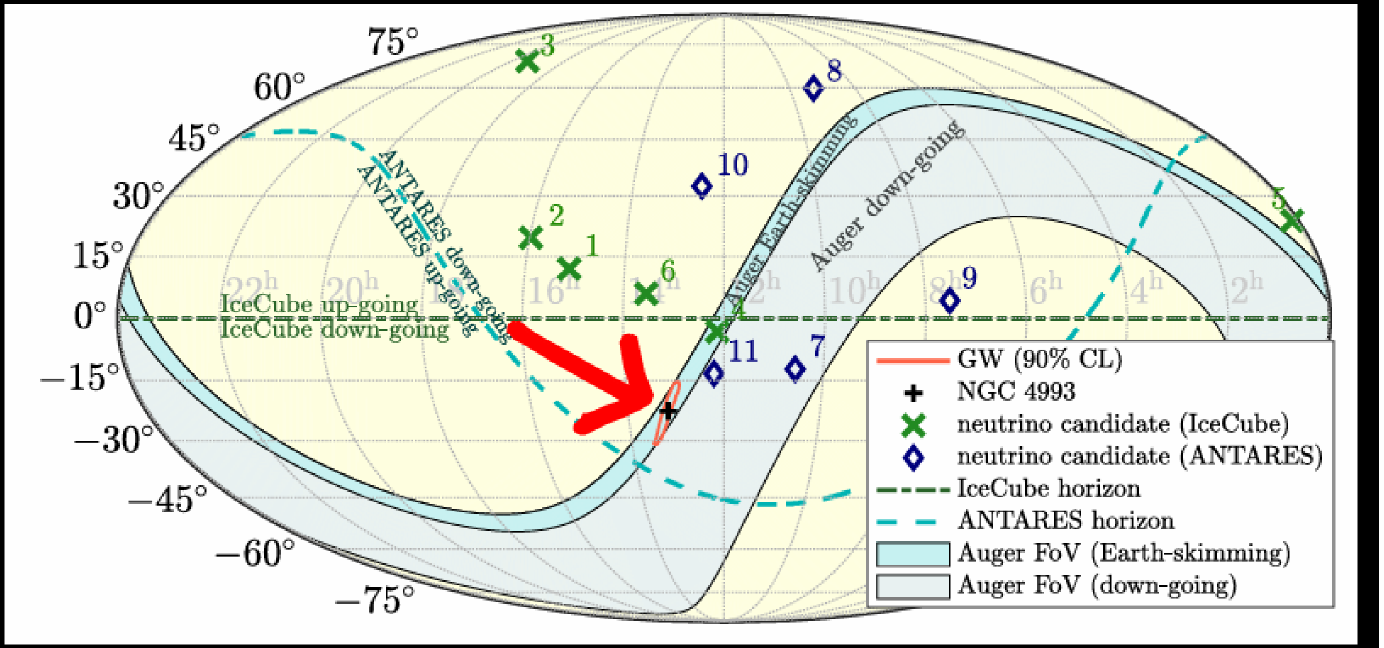

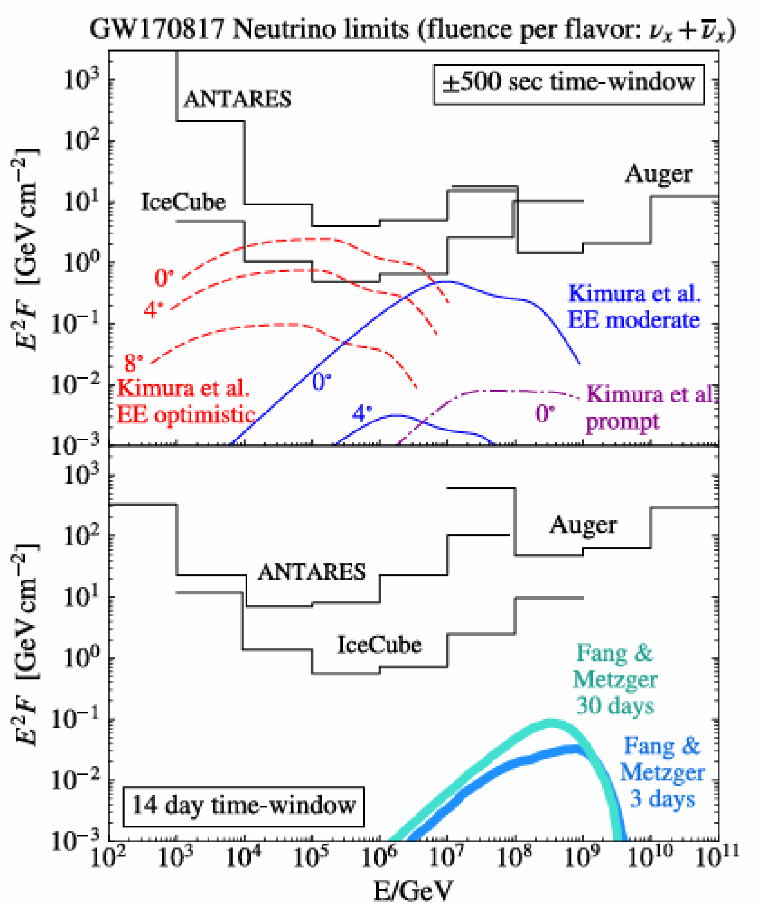

Typical off-axis GRB. Optimistic on-axis attenuated GRB constrained.

AUGER PHOTONS AND GRAVITATIONAL WAVES

UHE PHOTONS FROM GW SOURCES

ApJ 952 (2023) 91

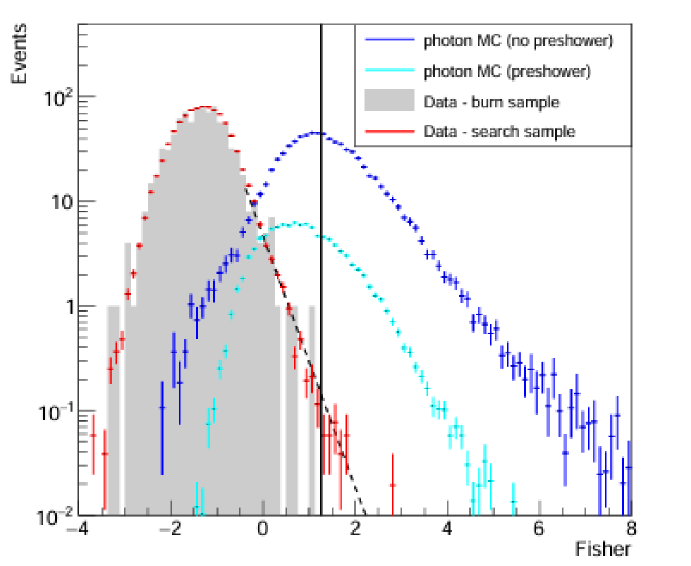

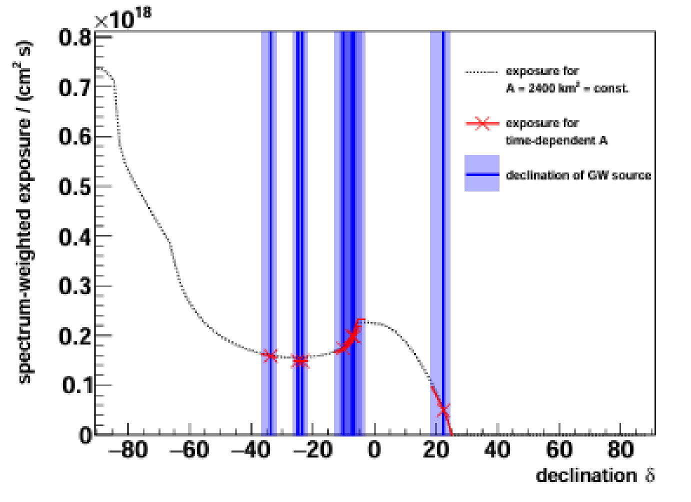

- Binary black hole (BBH)/neutron star (BNS) or black hole-neutron star (BHNS) mergers.
  - 10 events selected that maximize signal sensitivity and reduce background.
- BNS GW170817 (NGC4993) at 41 Mpc → $E^{UL}_{emit} < 0.04 M_\odot \left(E_\gamma > 2 \times 10^{19}\right)$ and $E^{UL}_{emit} < 0.008 M_\odot \left(E_\gamma > 4 \times 10^{19}\right)$

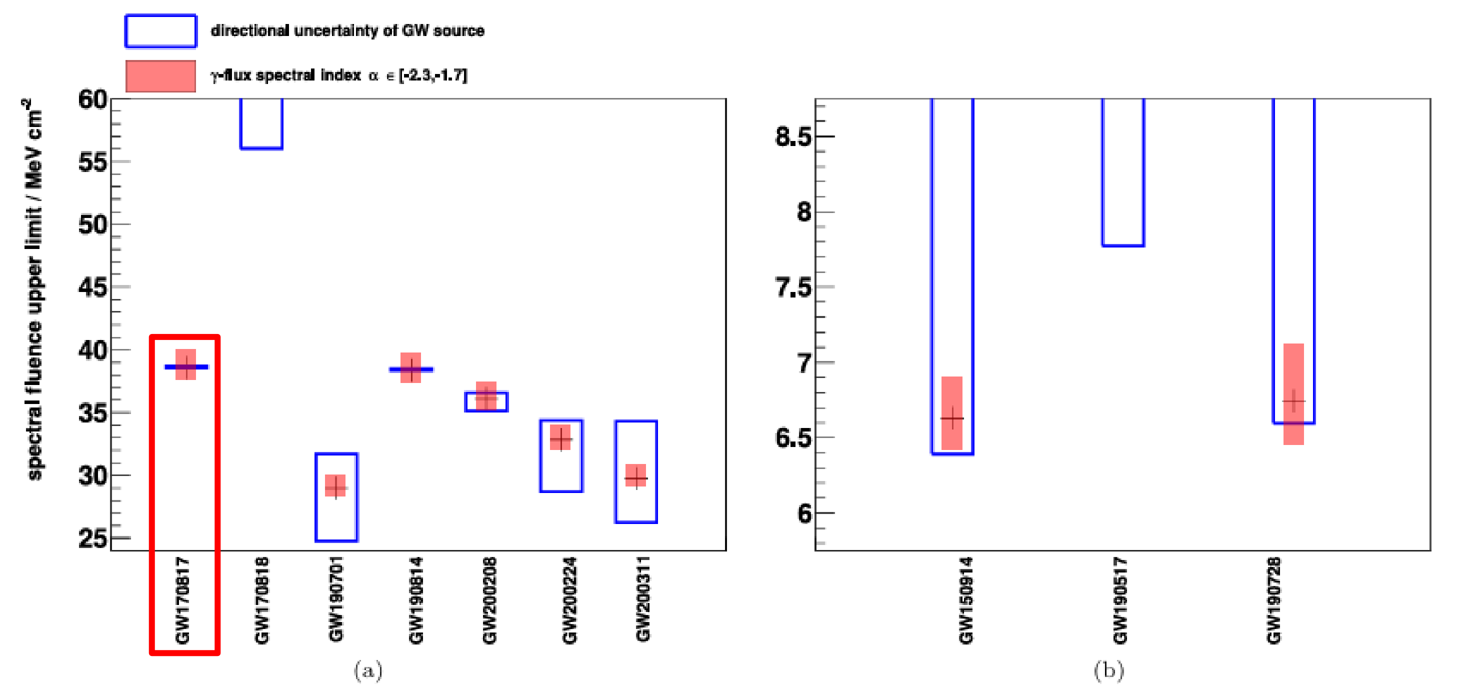

See Tim Fehler's ICNFP2024 talk
"Searches for ultra-high-energy photons with the Pierre Auger Observatory"

AUGER UHECR
CORRELATION WITH NEUTRINOS

CORRELATIONS OF NEUTRINOS WITH UHECR

ApJ 934 164 (2022)

Telescope Array	Pierre Auger	IceCube	ANTARES

Telescope Array

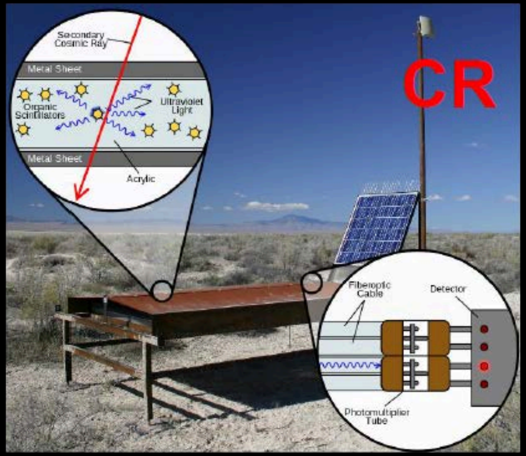

- Location: Utah Desert
- Surface Detector (SD) Array (507 scintillator detectors)
- 4 Fluorescence Detectors
- Exposure: Northern Hemisphere > 16⁰ Dec.

Pierre Auger

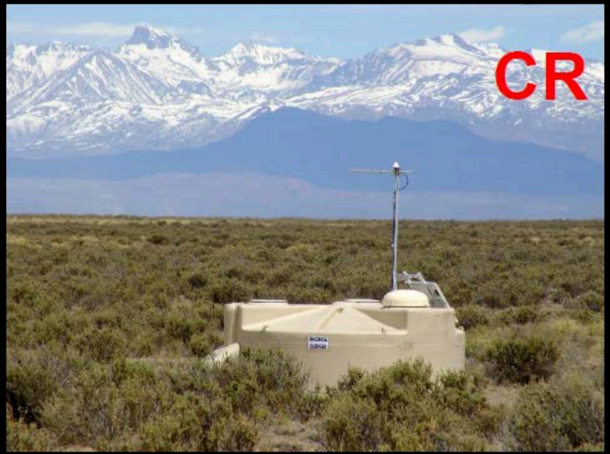

- Location: Argentina Desert
- SD Array (1660 water-Cherenkov detectors)
- 5 Fluorescence Detectors
- Exposure: Southern Hemisphere < 45⁰ Dec.

IceCube

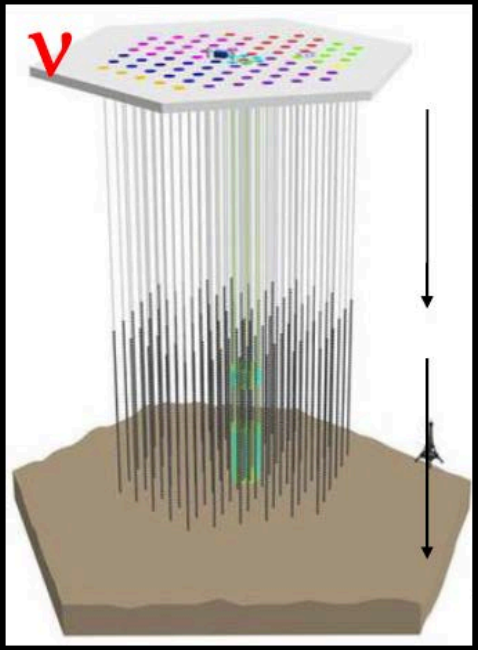

- Location: South Pole
- 86 Strings in Ice
- Each With 60 Digital Optical Modules

ANTARES

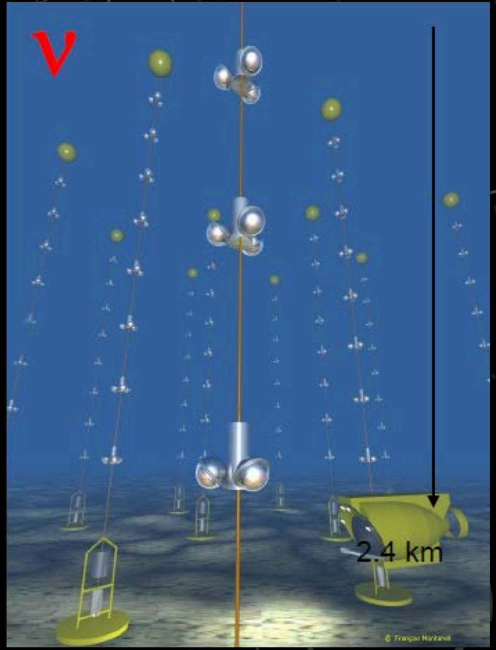

- Location: Mediterranean
- 12 Strings Anchored to Sea Floor
- 885 Optical Modules

1043 Authors

From A. Barbano: PoS(ICRC2019)842

CORRELATIONS OF NEUTRINOS WITH UHECR

ApJ 934 164 (2022)

Telescope Array

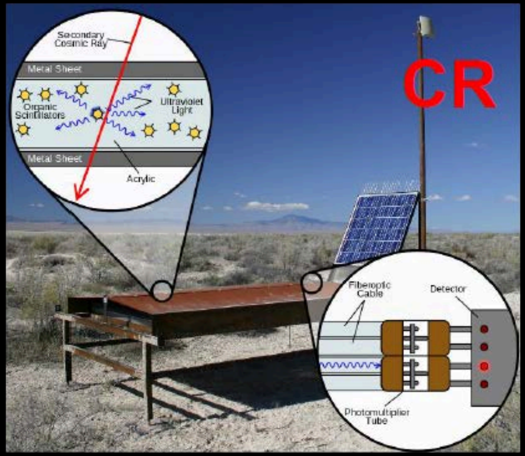

- Location: Utah Desert
- Surface Detector (SD) Array (507 scintillator detectors)
- 4 Fluorescence Detectors
- Exposure: Northern Hemisphere > 16⁰ Dec.

Pierre Auger

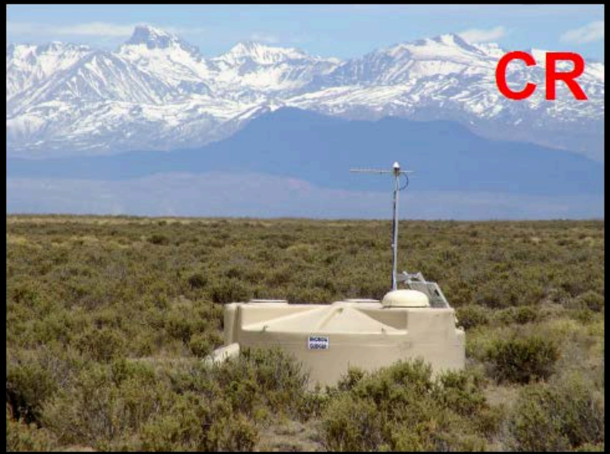

- Location: Argentina Desert
- SD Array (1660 water-Cherenkov detectors)
- 5 Fluorescence Detectors
- Exposure: Southern Hemisphere < 45⁰ Dec.

IceCube

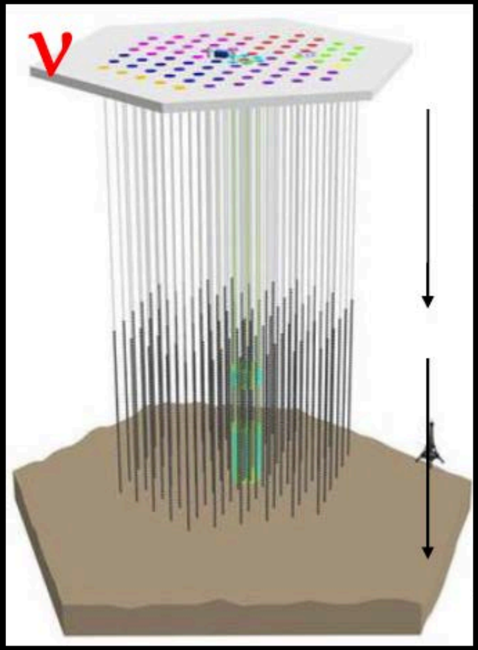

- Location: South Pole
- 86 Strings in Ice
- Each With 60 Digital Optical Modules

ANTARES

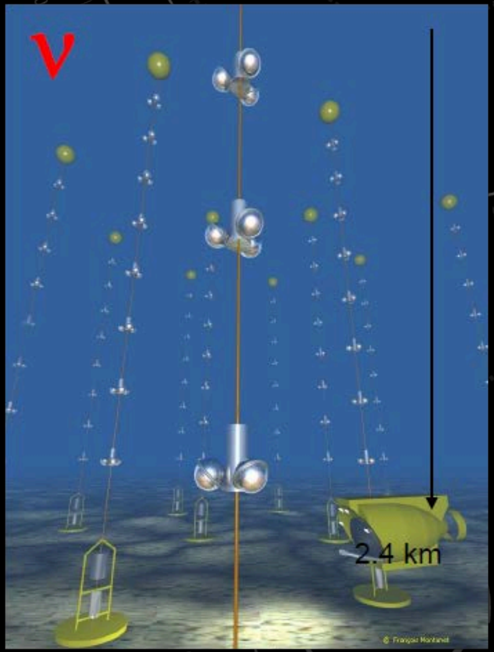

- Location: Mediterranean
- 12 Strings Anchored to Sea Floor
- 885 Optical Modules

1043 Authors

See Sonja Mayotte's ICNFP2024 talk
"The Pierre Auger Observatory as a Test Environment"

From A. Barbano: PoS(ICRC2019)842

CORRELATIONS OF NEUTRINOS WITH UHECR

ApJ 934 164 (2022)

- Three Analyses:
  1. Arrival direction cross-correlation between high-energy astrophysical neutrinos and UHECRS.
  - Two Stacked Likelihood Searches:
    2. UHECR excesses around HE neutrinos (“Neutrino Stacking”).
    3. Neutrino excesses around highest energy UHECR (“UHECR Stacking”).

CORRELATIONS OF NEUTRINOS WITH UHECR

ApJ 934 164 (2022)

- **Three Analyses:**
  1. **Arrival direction cross-correlation** between high-energy astrophysical neutrinos and UHECRS.
  - **Two Stacked Likelihood Searches:**
  2. **UHECR excesses around HE neutrinos ("Neutrino Stacking").**
  3. **Neutrino excesses around highest energy UHECR ("UHECR Stacking").**

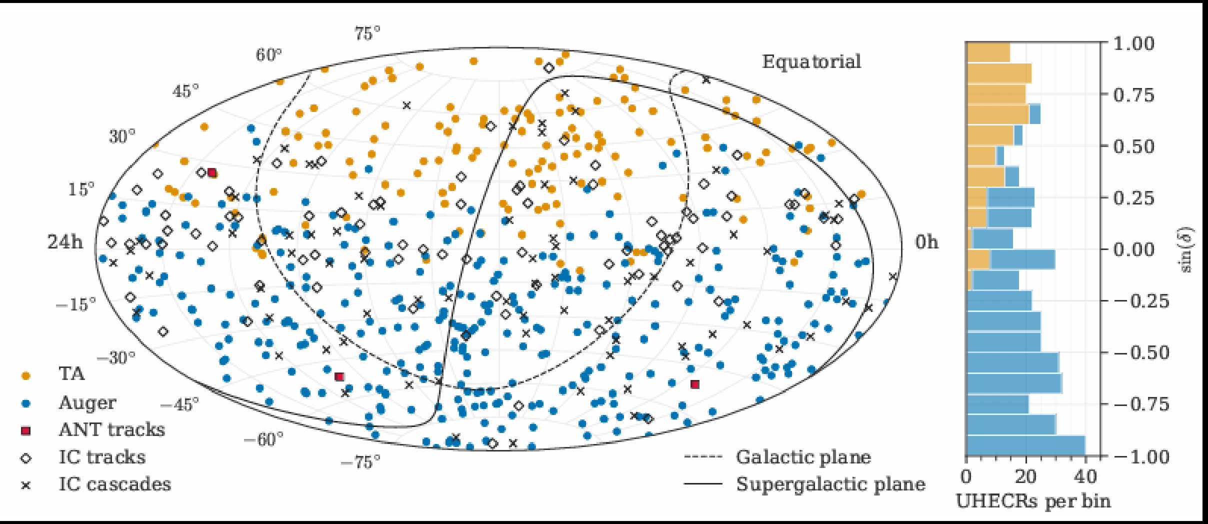

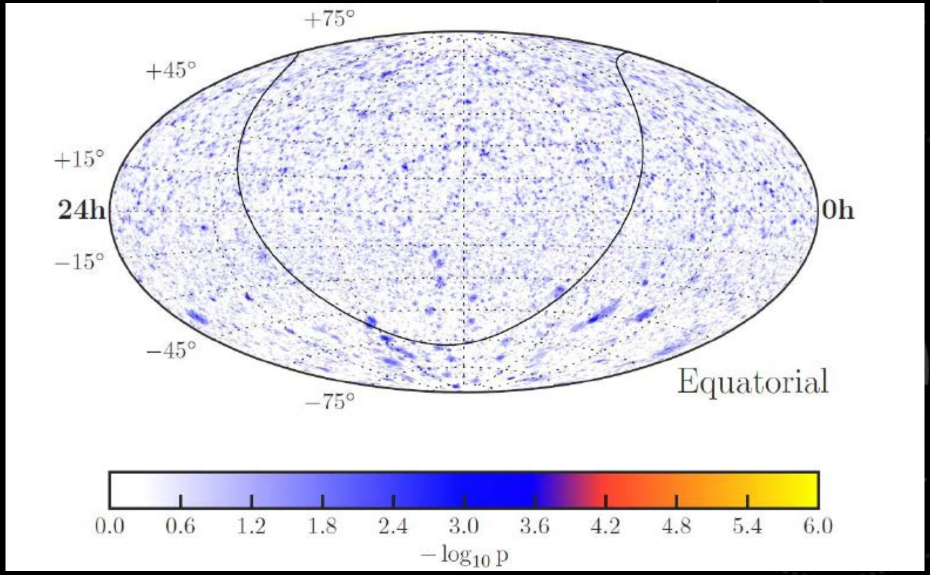

High-energy astrophysical neutrinos and UHECRS for 1.,2.

High Statistics IceCube 7-yr Point-Source Example for 3.

ARRIVAL DIRECTION CROSS-CORRELATION

ApJ 934 164 (2022)

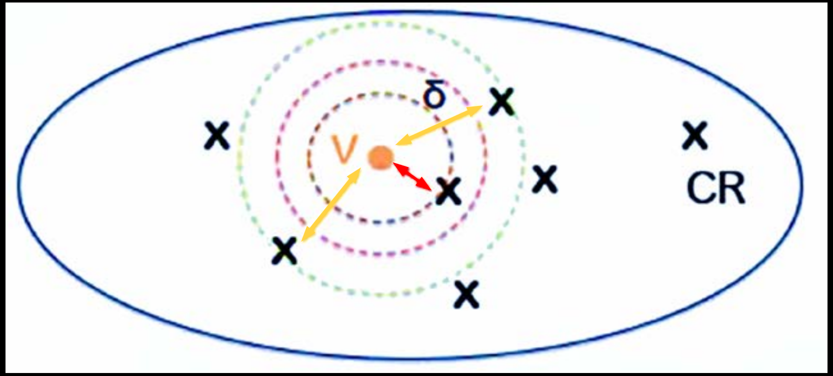

$1° < \delta < 30°, 1°$ steps

- n_{obs} = UHECR-neutrino pairs inside angular distance δ
- n_{exp} = Expected pairs under null-hypotheses:
    - i. Isotropic UHECR
    - ii. Isotropic Neutrinos

ARRIVAL DIRECTION CROSS-CORRELATION

ApJ 934 164 (2022)

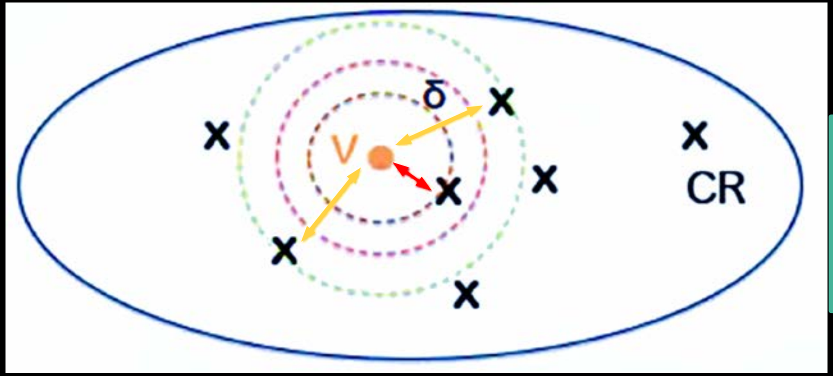

$1° < \delta < 30°, 1°$ steps

$$TS = max\left(\frac{n_{obs}(\delta)}{\langle n_{exp}(\delta)\rangle} - 1\right)$$

Isotropic MC

- n_{obs} = UHECR-neutrino pairs inside angular distance δ
- n_{exp} = Expected pairs under null-hypotheses:
  i. Isotropic UHECR
  ii. Isotropic Neutrinos

ARRIVAL DIRECTION CROSS-CORRELATION

ApJ 934 164 (2022)

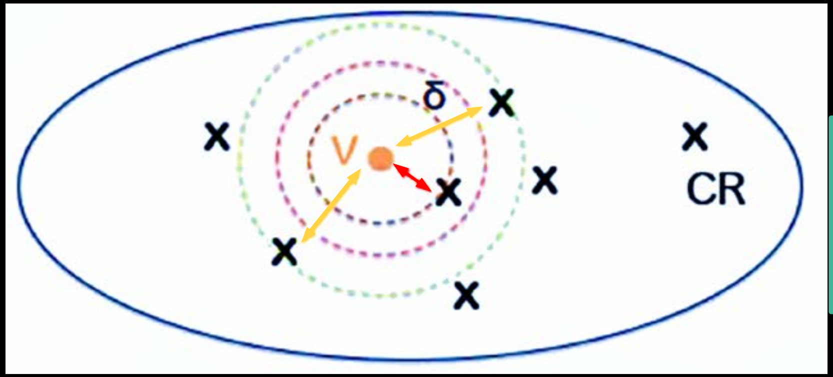

$1° < \delta < 30°$, $1°$ steps

$$TS = max\left(\frac{n_{obs}(\delta)}{\langle n_{exp}(\delta)\rangle} - 1\right)$$

- n_{obs} = UHECR-neutrino pairs inside angular distance δ
- n_{exp} = Expected pairs under null-hypotheses:
  1. Isotropic UHECR
  2. Isotropic Neutrinos (most significant)

Compatible with Backgrounds

- Isotropic Neutrinos:
  - Randomized neutrinos.
  - UHECR data fixed.

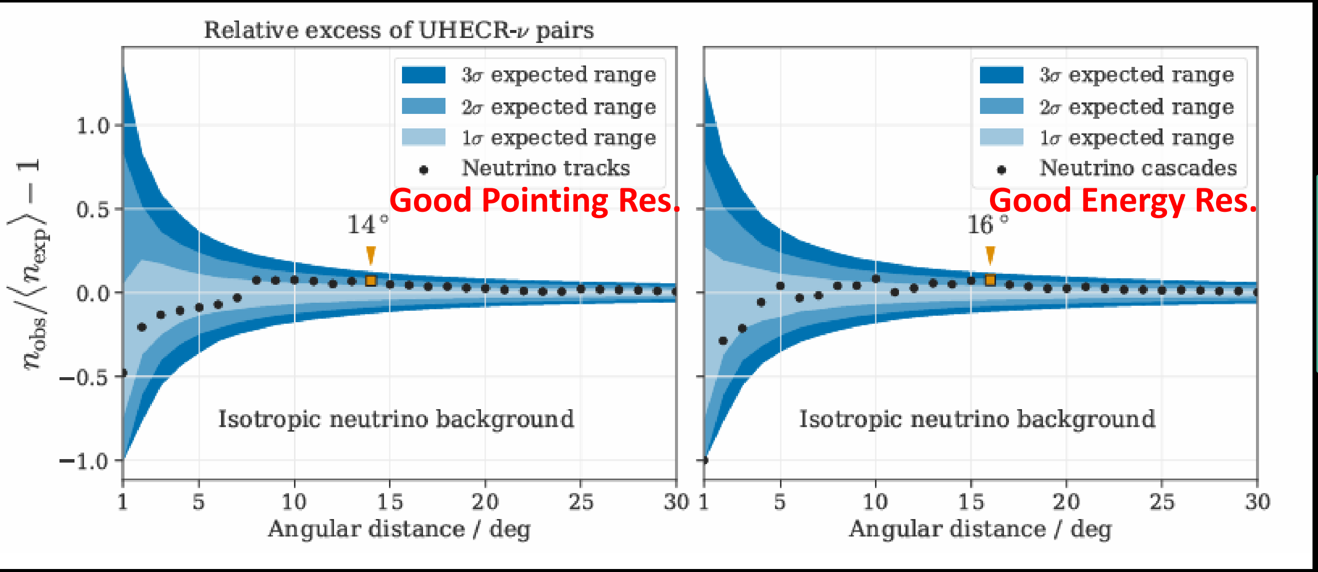

- Post-trial p-vals (δ scan):
  - Tracks: 0.23
  - Cascades: 0.15

UHECR EXCESS AROUND HE NEUTRINO SOURCES

ApJ 934 164 (2022)

- **Hypotheses:**
  - **Signal: Astrophysical neutrino as source location with correlated UHECR.**
  - **Background: *Isotropic UHECR*.**

$$\ln \mathcal{L}(n_s) = \sum_{i=1}^{N_{Auger}} \ln\left(\frac{n_s}{N_{CR}} S^i_{Auger} + \frac{N_{CR} - n_s}{N_{CR}} B^i_{Auger}\right) + \sum_{i=1}^{N_{TA}} \ln\left(\frac{n_s}{N_{CR}} S^i_{TA} + \frac{N_{CR} - n_s}{N_{CR}} B^i_{TA}\right)$$

UHECR EXCESS AROUND HE NEUTRINO SOURCES

ApJ 934 164 (2022)

- **Hypotheses:**
  - **Signal: Astrophysical neutrino as source location with correlated UHECR.**
  - **Background: Isotropic UHECR.**

$$\ln \mathcal{L}(n_s) = \sum_{i=1}^{N_{Auger}} \ln\left(\frac{n_s}{N_{CR}} S^i_{Auger} + \frac{N_{CR} - n_s}{N_{CR}} B^i_{Auger}\right) + \sum_{i=1}^{N_{TA}} \ln\left(\frac{n_s}{N_{CR}} S^i_{TA} + \frac{N_{CR} - n_s}{N_{CR}} B^i_{TA}\right)$$

- n_s: **# signal UHECR (free param.)**
- $N_{CR} = N_{TA} + N_{Auger}$
- S^i_{det}: **UHECR event i signal prob.**
- B^i_{det}: **Event i background prob.**

UHECR EXCESS AROUND HE NEUTRINO SOURCES

ApJ 934 164 (2022)

- Hypotheses:
  - Signal: Astrophysical neutrino as source location with correlated UHECR.
  - Background: Isotropic UHECR.

$$\ln \mathcal{L}(n_s) = \sum_{i=1}^{N_{Auger}} \ln\left(\frac{n_s}{N_{CR}} S^i_{Auger} + \frac{N_{CR} - n_s}{N_{CR}} B^i_{Auger}\right) + \sum_{i=1}^{N_{TA}} \ln\left(\frac{n_s}{N_{CR}} S^i_{TA} + \frac{N_{CR} - n_s}{N_{CR}} B^i_{TA}\right)$$

- n_s: # signal UHECR (free param.)
- $N_{CR} = N_{TA} + N_{Auger}$
- S^i_{det}: UHECR event i signal prob.
- B^i_{det}: Event i background prob.

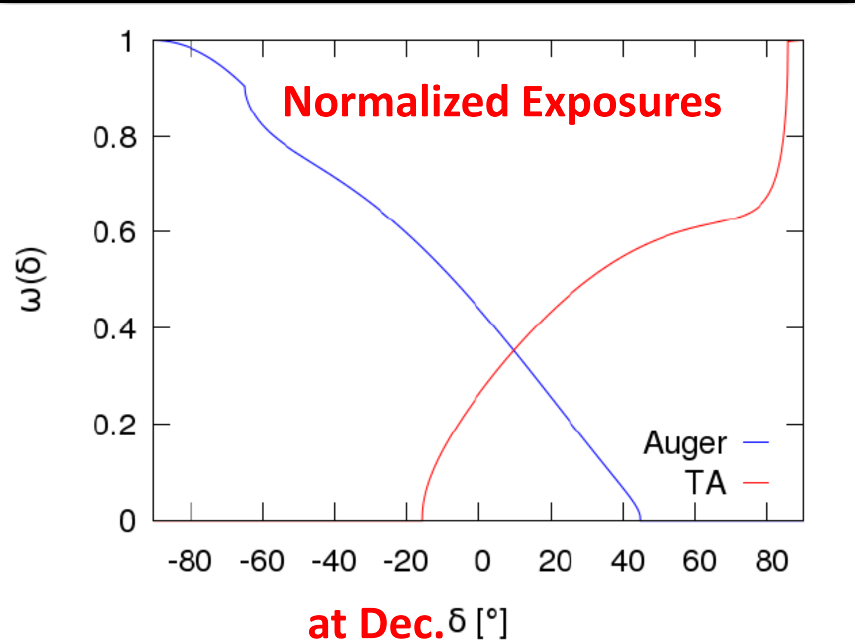

Background PDF $B_{det}(\delta)$ or Relative Exposure $R_{det}(\delta)$

UHECR EXCESS AROUND HE NEUTRINO SOURCES

ApJ 934 164 (2022)

- **Hypotheses:**
  - **Signal: Astrophysical neutrino as source location with correlated UHECR.**
  - **Background: Isotropic UHECR.**

$$\ln \mathcal{L}(n_s) = \sum_{i=1}^{N_{Auger}} \ln\left(\frac{n_s}{N_{CR}} S^i_{Auger} + \frac{N_{CR} - n_s}{N_{CR}} B^i_{Auger}\right) + \sum_{i=1}^{N_{TA}} \ln\left(\frac{n_s}{N_{CR}} S^i_{TA} + \frac{N_{CR} - n_s}{N_{CR}} B^i_{TA}\right)$$

- **n_s: # signal UHECR (free param.)**
- **$N_{CR} = N_{TA} + N_{Auger}$**
- **S^i_{det}: UHECR event i signal prob.**
- **B^i_{det}: Event i background prob.**

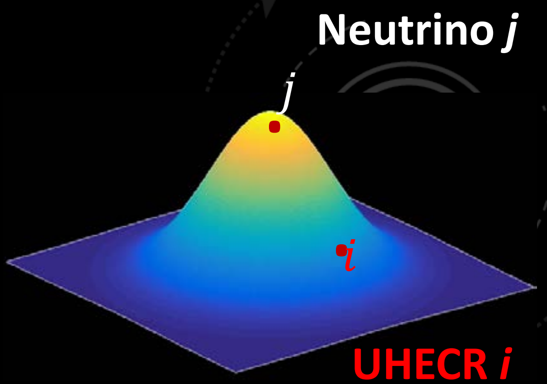

UHECR EXCESS AROUND HE NEUTRINO SOURCES

ApJ 934 164 (2022)

- **Hypotheses:**
  - **Signal:** Astrophysical neutrino as source location with correlated UHECR.
  - **Background:** Isotropic UHECR.

Signal and Background Proportions

$$\ln \mathcal{L}(n_s) = \sum_{i=1}^{N_{Auger}} \ln\left(\frac{n_s}{N_{CR}} S^i_{Auger} + \frac{N_{CR} - n_s}{N_{CR}} B^i_{Auger}\right) + \sum_{i=1}^{N_{TA}} \ln\left(\frac{n_s}{N_{CR}} S^i_{TA} + \frac{N_{CR} - n_s}{N_{CR}} B^i_{TA}\right)$$

- n_s: # signal UHECR (free param.)
- $N_{CR} = N_{TA} + N_{Auger}$
- S^i_{det}: UHECR event i signal prob.
- B^i_{det}: Event i background prob.

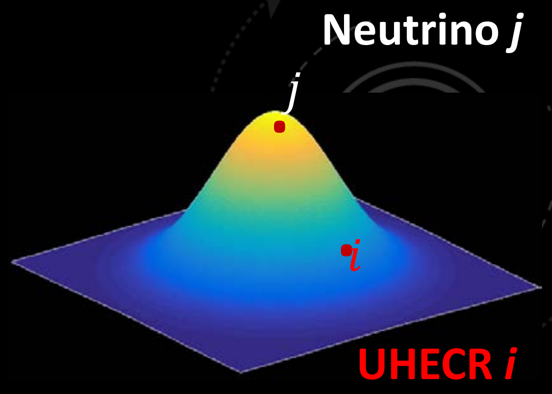

UHECR EXCESS AROUND HE NEUTRINO SOURCES

ApJ 934 164 (2022)

- **Hypotheses:**
  - **Signal: Astrophysical neutrino as source location with correlated UHECR.**
  - **Background: Isotropic UHECR.**

$$\ln \mathcal{L}(n_s) = \sum_{i=1}^{N_{Auger}} \ln\left(\frac{n_s}{N_{CR}} S^i_{Auger} + \frac{N_{CR}-n_s}{N_{CR}} B^i_{Auger}\right) + \sum_{i=1}^{N_{TA}} \ln\left(\frac{n_s}{N_{CR}} S^i_{TA} + \frac{N_{CR}-n_s}{N_{CR}} B^i_{TA}\right)$$

- n_s: # signal UHECR (free param.)
- $N_{CR} = N_{TA} + N_{Auger}$
- S^i_{det}: UHECR event i signal prob.
- B^i_{det}: Event i background prob.

$$S^i_{det}(\delta_i, E_i) = R_{det}(\delta_i) \sum_{j=1}^{N_{src,\nu}} S_{ij}\left(\vec{\Omega}_i, \sigma_i(E_i)\right)$$

$$\sigma_i(E_i) = \sqrt{\sigma^2_{det} + \sigma(E_i)^2_{MD}}$$

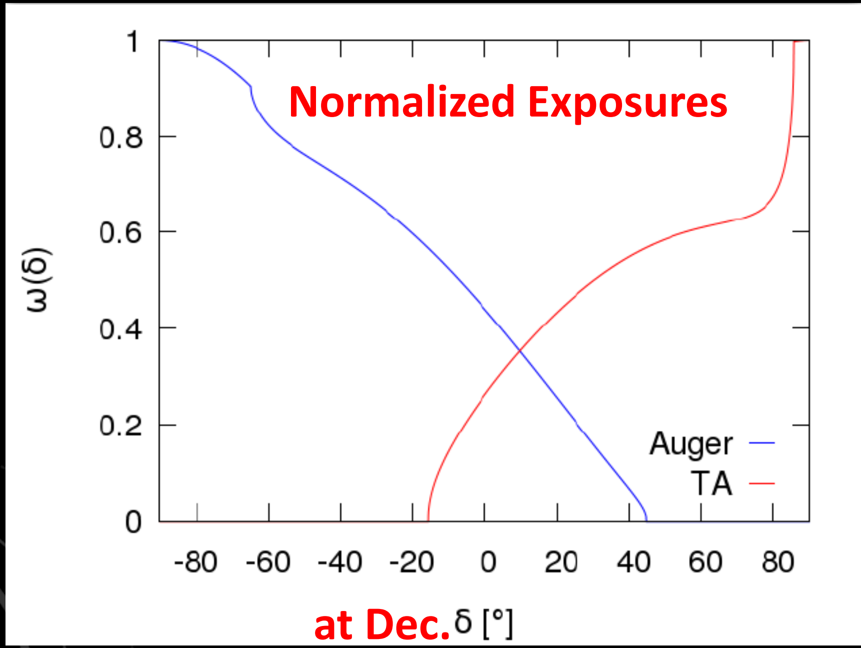

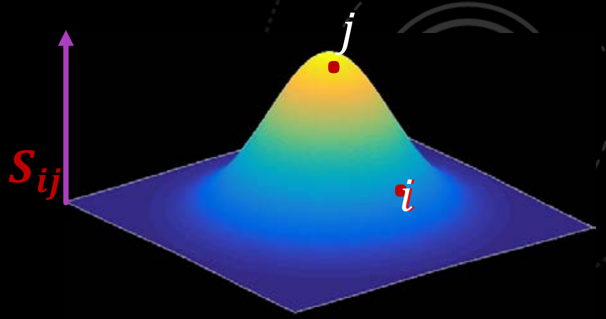

Background PDF $B_{det}(\delta)$ or Relative Exposure $R_{det}(\delta)$

UHECR EXCESS AROUND HE NEUTRINO SOURCES

ApJ 934 164 (2022)

- **Hypotheses:**
  - **Signal: Astrophysical neutrino as source location with correlated UHECR.**
  - **Background: Isotropic UHECR.**

$$\ln \mathcal{L}(n_s) = \sum_{i=1}^{N_{Auger}} \ln\left(\frac{n_s}{N_{CR}} S^i_{Auger} + \frac{N_{CR}-n_s}{N_{CR}} B^i_{Auger}\right) + \sum_{i=1}^{N_{TA}} \ln\left(\frac{n_s}{N_{CR}} S^i_{TA} + \frac{N_{CR}-n_s}{N_{CR}} B^i_{TA}\right)$$

- n_s: # signal UHECR (free param.)
- $N_{CR} = N_{TA} + N_{Auger}$
- S^i_{det}: UHECR event i signal prob.
- B^i_{det}: Event i background prob.

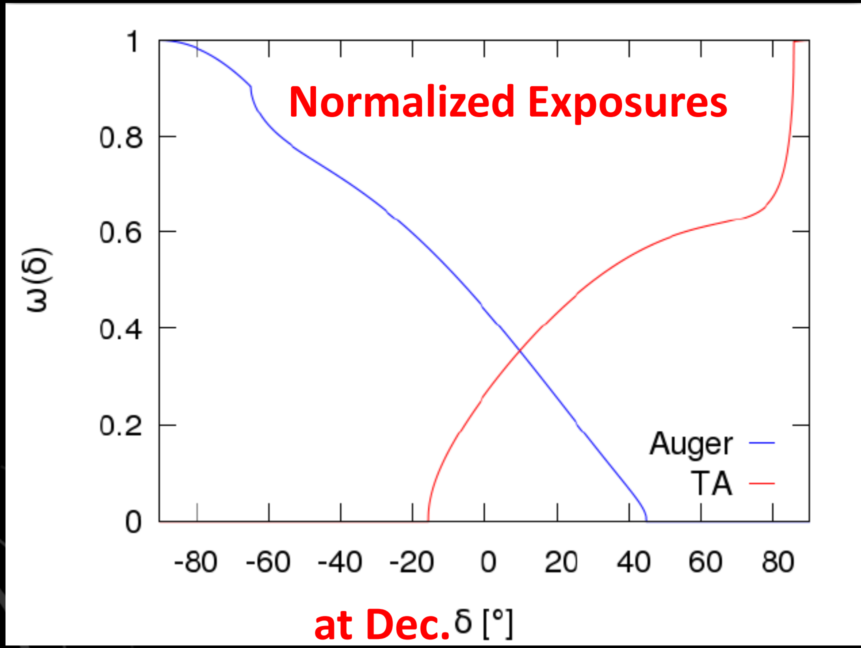

Background PDF $B_{det}(\delta)$ or Relative Exposure $R_{det}(\delta)$

$$S^i_{det}(\delta_i, E_i) = R_{det}(\delta_i) \sum_{j=1}^{N_{src,\nu}} S_{ij}\left(\vec{\Omega}_i, \sigma_i(E_i)\right)$$

$$\sigma_i(E_i) = \sqrt{\sigma^2_{det} + \sigma(E_i)^2_{MD}}$$

- S_{ij}: Gaussian around ν source j
- σ_{det}: Angular Resolution
- σ_{MD}: Magnetic Deflection

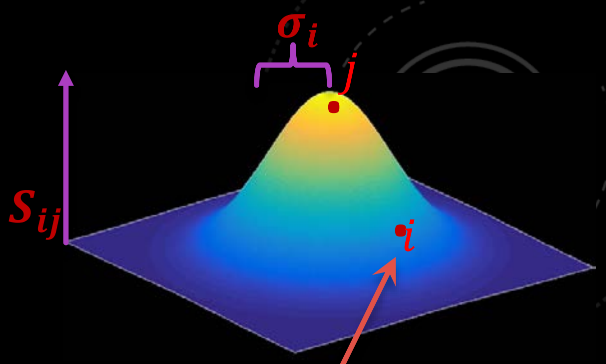

$\vec{\Omega}_i$: UHECR Pointing-direction.

UHECR EXCESS AROUND HE NEUTRINO SOURCES

ApJ 934 164 (2022)

- **Hypotheses:**
  - **Signal: Astrophysical neutrino as source location with correlated UHECR.**
  - **Background: Isotropic UHECR.**

$$TS = -2 \ln \left(\frac{\mathcal{L}(\hat{n}_s)}{\mathcal{L}(n_s = 0)} \right)$$

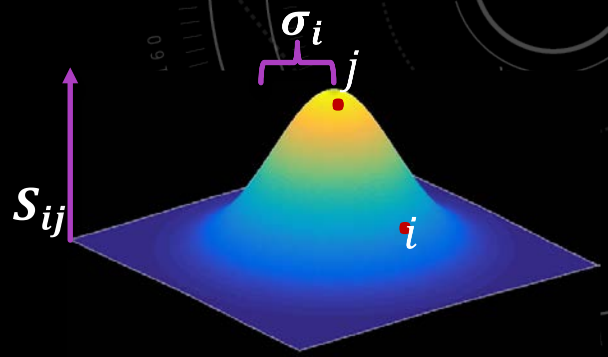

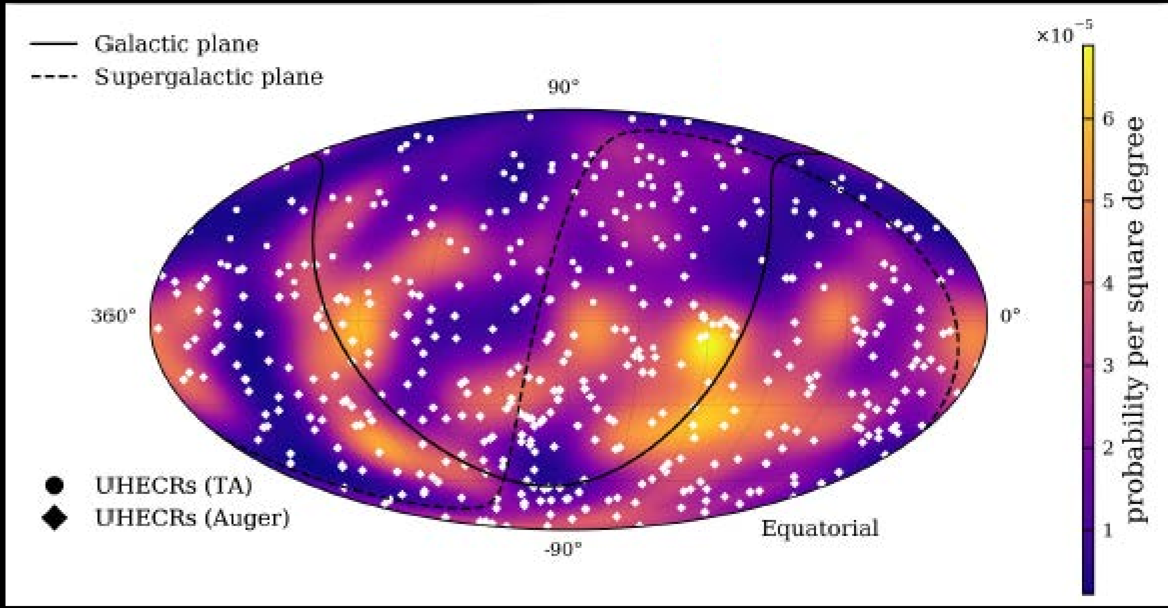

Stacked likelihood map of neutrino shower-like events and UHECR arrival directions

UHECR EXCESS AROUND HE NEUTRINO SOURCES

ApJ 934 164 (2022)

- **Hypotheses:**
  - **Signal: Astrophysical neutrino as source location with correlated UHECR.**
  - **Background: Isotropic UHECR.**

$$TS = -2\ln\left(\frac{\mathcal{L}(\hat{n}_s)}{\mathcal{L}(n_s = 0)}\right)$$

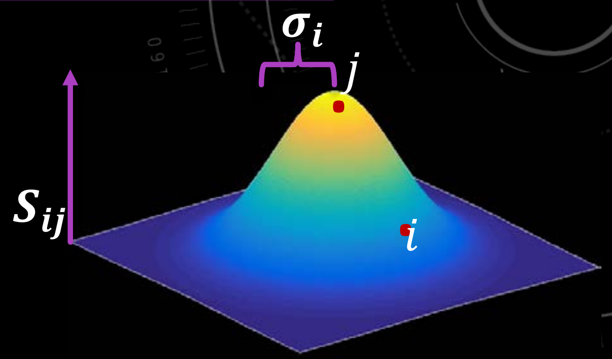

Pre-trial

p-values			
tracks	>0.5	>0.5	>0.5
cascades	>0.5	0.38	0.26

3 magnetic deflections $\sigma_{MD} = D * \frac{100\ EeV}{E}$ tested

Results consistent with isotropic UHECR

- **Uncertainties in Compositions and Magnetic Fields**

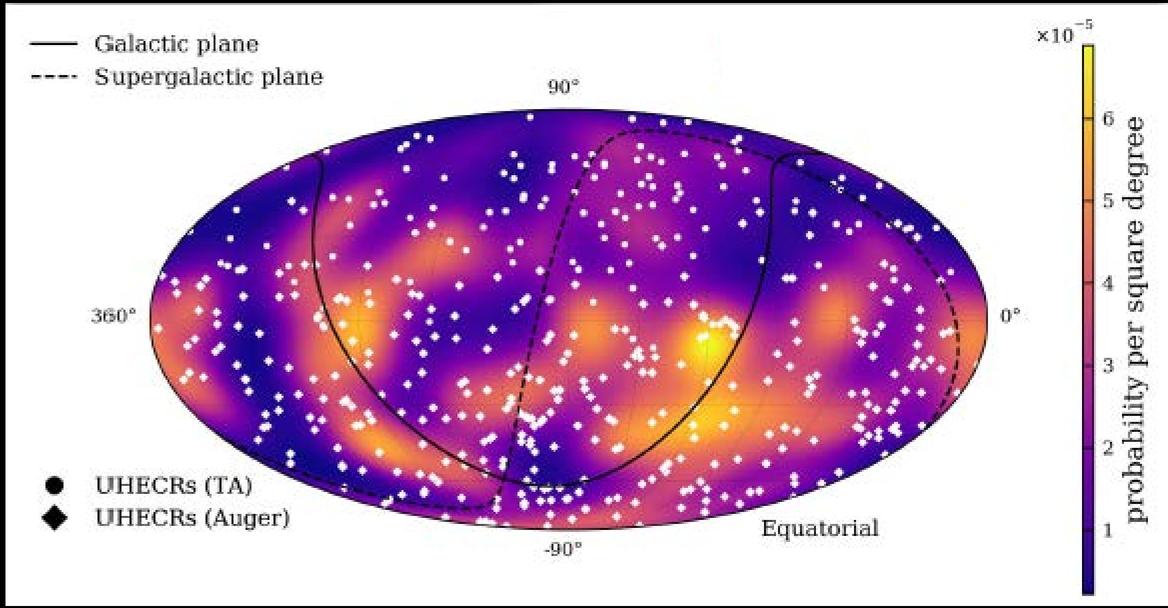

Stacked likelihood map of neutrino shower-like events and UHECR arrival directions

NEUTRINO EXCESS AROUND HIGHEST ENERGY CR SOURCES

ApJ 934 164 (2022)

- **Hypotheses:**
  - Signal: Highest energy UHECR as source locations with correlated ν.
  - Background: *Isotropic* ν.

$$\ln \mathcal{L}(n_s, \gamma_s) = \sum_{j=1}^{N_{CR}} \left[\left(\sum_{i=1}^{N_\nu} \ln \left(\frac{n_s}{N_\nu} S_\nu^i(\gamma_s, \vec{\Omega}_s) + \frac{N_\nu - n_s}{N_\nu} B_\nu^i(\vec{\Omega}_s) \right) \right) - \frac{\left(\vec{\Omega}_s - \vec{\Omega}_j\right)^2}{\sigma_j(E_j)^2} \right]$$

- n_s: # signal events (free param.)
- γ_s: ν source spectrum index (free param.)
- S_ν^i: ν event i signal prob.
- B_ν^i: Event i background prob.
- $\vec{\Omega}_s$: Pointing-direction of grid point.

NEUTRINO EXCESS AROUND HIGHEST ENERGY CR SOURCES

ApJ 934 164 (2022)

Step One

$$\ln \mathcal{L}(n_s, \gamma_s) = \sum_{j=1}^{N_{CR}} \left[\left(\sum_{i=1}^{N_\nu} \ln \left(\frac{n_s}{N_\nu} S_\nu^i(\gamma_s, \vec{\Omega}_s) + \frac{N_\nu - n_s}{N_\nu} B_\nu^i(\vec{\Omega}_s) \right) \right) - \frac{\left(\vec{\Omega}_s - \vec{\Omega}_j\right)^2}{\sigma_j(E_j)^2} \right]$$

- **Hypotheses:**
  - **Signal:** Highest energy UHECR as source locations with correlated ν.
  - **Background:** Isotropic ν.

- n_s: # signal events (free param.)
- γ_s: ν source spectrum index (free param.)
- S_ν^i: ν event i signal prob.
- B_ν^i: Event i background prob.
- $\vec{\Omega}_s$: Pointing-direction of grid point.

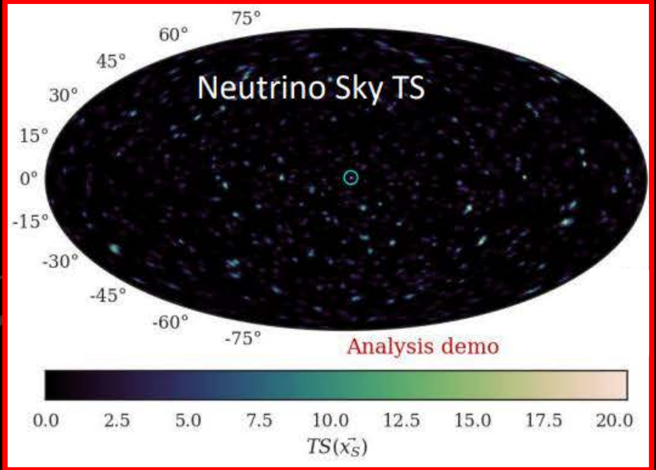

$$TS(\vec{\Omega}_s) = 2 \ln \left(\frac{\mathcal{L}_1(\hat{n}_s, \hat{\gamma}_s)}{\mathcal{L}_1(n_s = 0)} \right)$$

NEUTRINO EXCESS AROUND HIGHEST ENERGY CR SOURCES

ApJ 934 164 (2022)

- **Hypotheses:**
  - **Signal:** Highest energy UHECR as source locations with correlated ν.
  - **Background:** Isotropic ν.

Step Two

$$\ln \mathcal{L}(n_s, \gamma_s) = \sum_{j=1}^{N_{CR}} \left[\left(\sum_{i=1}^{N_\nu} \ln \left(\frac{n_s}{N_\nu} S_\nu^i(\gamma_s, \vec{\Omega}_s) + \frac{N_\nu - n_s}{N_\nu} B_\nu^i(\vec{\Omega}_s) \right) \right) - \frac{\left(\vec{\Omega}_s - \vec{\Omega}_j\right)^2}{\sigma_j(E_j)^2} \right]$$

- n_s: # signal events (free param.)
- γ_s: ν source spectrum index (free param.)
- S_ν^i: ν event i signal prob.
- B_ν^i: Event i background prob.
- $\vec{\Omega}_s$: Pointing-direction of grid point.

$\propto \ln(Gaussian)$

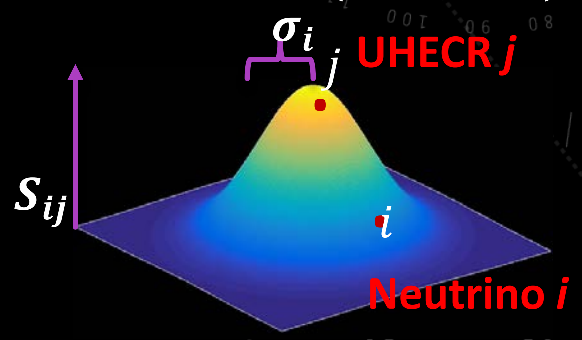

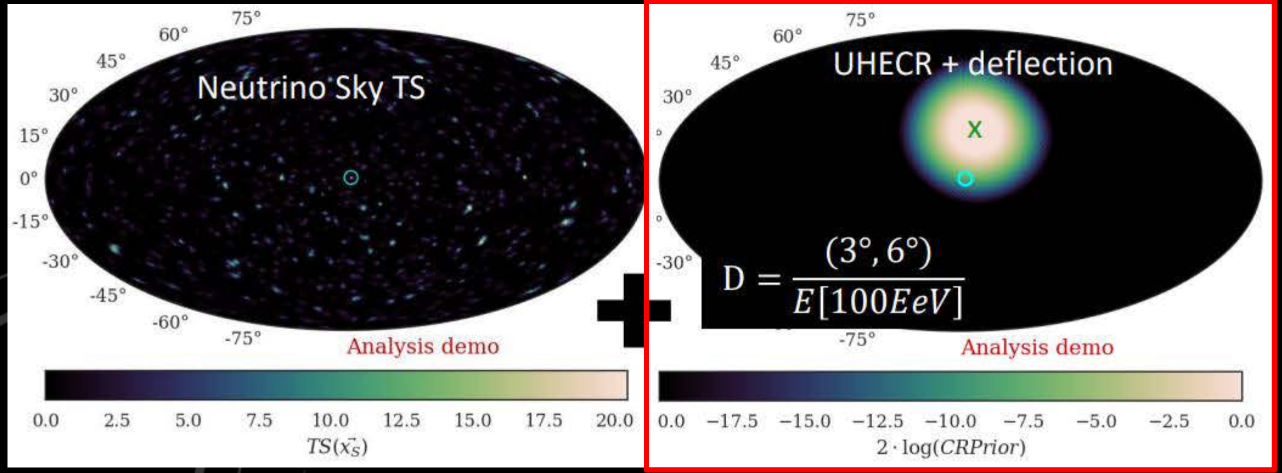

NEUTRINO EXCESS AROUND HIGHEST ENERGY CR SOURCES

ApJ 934 164 (2022)

Step Three

$$\ln \mathcal{L}(n_s, \gamma_s) = \sum_{j=1}^{N_{CR}} \left[\left(\sum_{i=1}^{N_\nu} \ln \left(\frac{n_s}{N_\nu} S_\nu^i(\gamma_s, \vec{\Omega}_s) + \frac{N_\nu - n_s}{N_\nu} B_\nu^i(\vec{\Omega}_s) \right) \right) - \frac{\left(\vec{\Omega}_s - \vec{\Omega}_j\right)^2}{\sigma_j(E_j)^2} \right]$$

- **Hypotheses:**
  - **Signal:** Highest energy UHECR as source locations with correlated ν.
  - **Background:** Isotropic ν.

- n_s: # signal events (free param.)
- γ_s: ν source spectrum index (free param.)
- S_ν^i: ν event i signal prob.
- B_ν^i: Event i background prob.
- $\vec{\Omega}_s$: Pointing-direction of grid point.

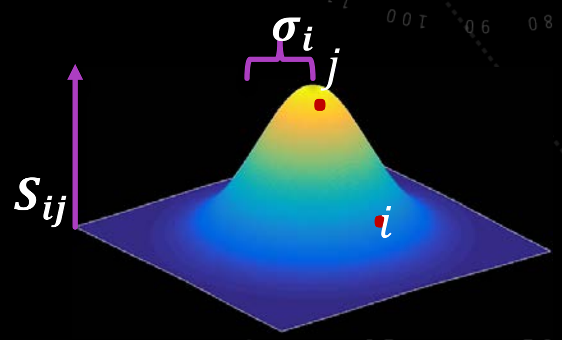

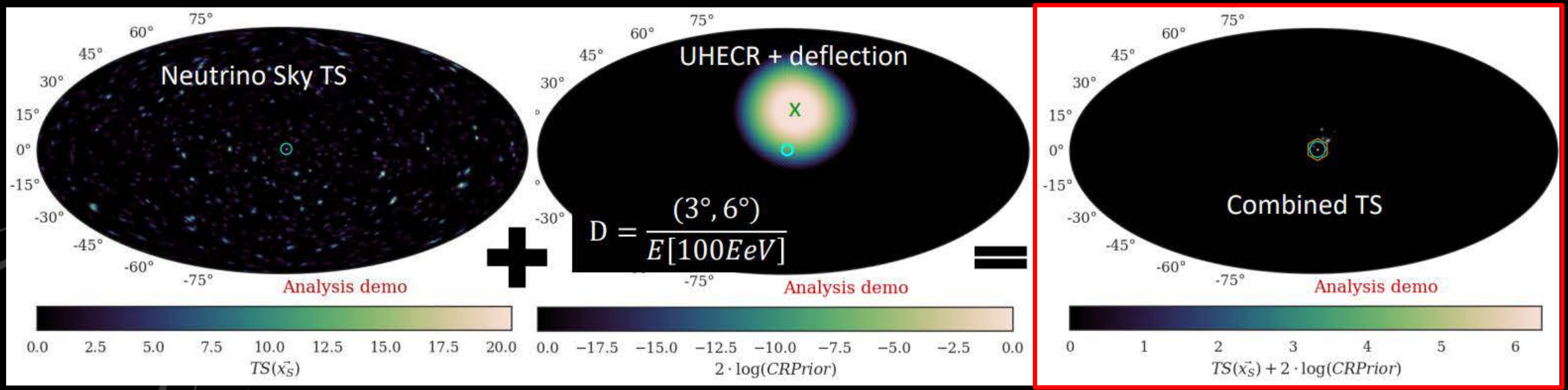

Grid point $\vec{\Omega}_s$ appears as hottest ν source corresponding to CR j

NEUTRINO EXCESS AROUND HIGHEST ENERGY CR SOURCES

ApJ 934 164 (2022)

Step Four

$$\ln \mathcal{L}(n_s, \gamma_s) = \sum_{j=1}^{N_{CR}} \left[\left(\sum_{i=1}^{N_\nu} \ln \left(\frac{n_s}{N_\nu} S_\nu^i(\gamma_s, \vec{\Omega}_s) + \frac{N_\nu - n_s}{N_\nu} B_\nu^i(\vec{\Omega}_s) \right) \right) - \frac{\left(\vec{\Omega}_s - \vec{\Omega}_j\right)^2}{\sigma_j(E_j)^2} \right]$$

- **Hypotheses:**
  - **Signal:** Highest energy UHECR as source locations with correlated ν.
  - **Background:** Isotropic ν.

- n_s: # signal events (free param.)
- γ_s: ν source spectrum index (free param.)
- S_ν^i: ν event i signal prob.
- B_ν^i: Event i background prob.
- $\vec{\Omega}_s$: Pointing-direction of grid point.

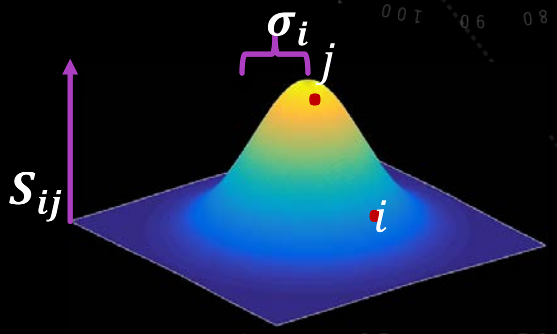

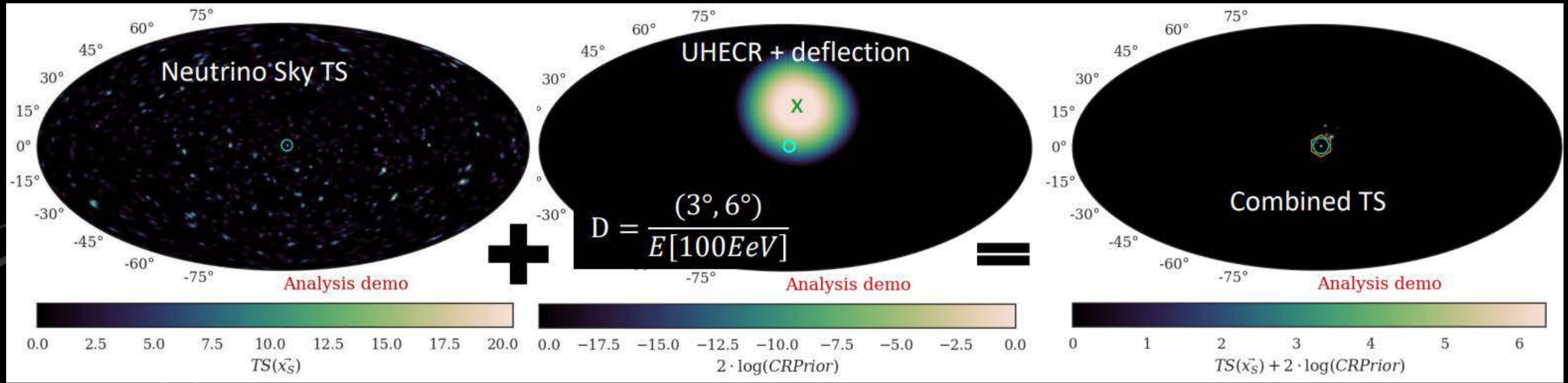

Grid point $\vec{\Omega}_s$ appears as hottest ν source corresponding to CR j:
Sum For All CRs

NEUTRINO EXCESS AROUND HIGHEST ENERGY CR SOURCES

ApJ 934 164 (2022)

- **Hypotheses:**
  - **Signal: Highest energy UHECR as source locations with correlated ν.**
  - **Background: Isotropic ν.**

Different magnetic deflections and UHECR energy cutoffs

Analysis parameters						
$D_0 \cdot C$	3°	3°	3°	6°	6°	6°
$E_{\rm cut}$	70 EeV	85 EeV	100 EeV	70 EeV	85 EeV	100 EeV
Pre-trial p-value	0.33	0.23	>0.5	0.19	0.097	0.43

~0.2 post-trial

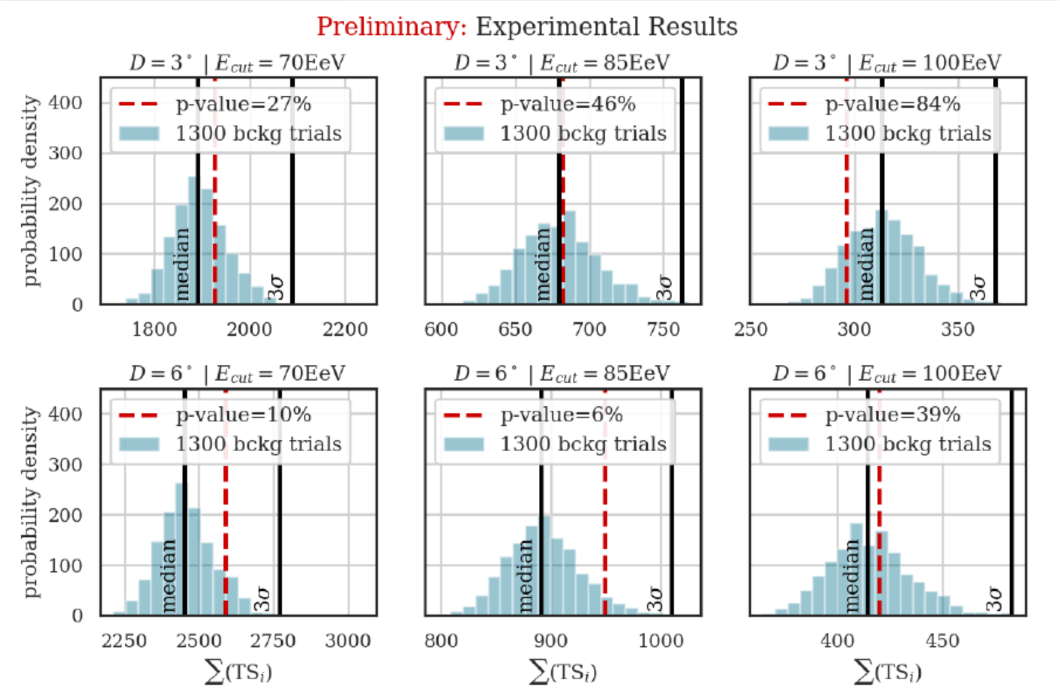

Results consistent with isotropic neutrinos

- **Uncertainties in Compositions and Magnetic Fields**

AUGER NEUTRONS
CORRELATION WITH GALACTIC GAMMA-RAYS

NEUTRONS AND GALACTIC GAMMA-RAYS

PoS (ICRC2023) 246

- Neutrons generated by UHECR i.e. photodisintegration and pion-production.
- Neutral particles point directly to sources -- no magnetic deflection.
- Mean lifetime of 15 minutes → $\langle Distance \rangle = 9.2\ kpc \times \frac{E_N}{EeV}$ (galactic scale)
- Extensive air showers: protons and neutrons are indistinguishable.
- Neutron fluxes may be found by excess of UHECR around possible source.

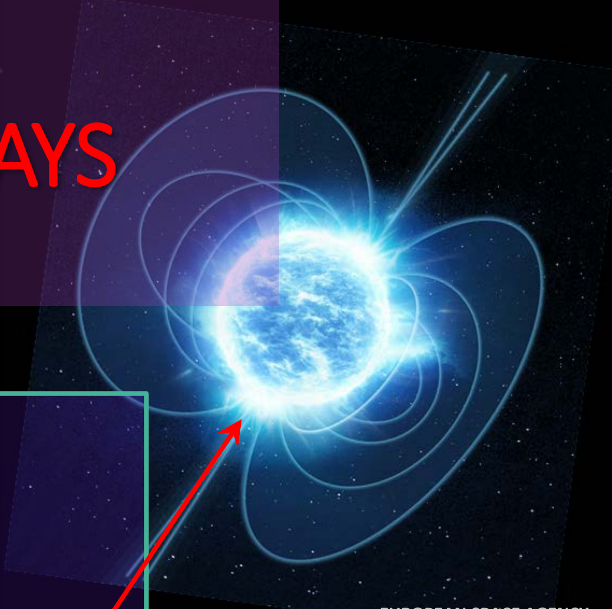

EUROPEAN SPACE AGENCY

RYUUNOSUKE TAKESHIGE

GAMMA TARGET CR PROBABILITY DENSITY

PoS (ICRC2023) 246

- CR event i weight equal to probability of originating at source j

$$w_{ij} = \frac{1}{2\pi\sigma_i^2} e^{-\frac{\xi_{ij}^2}{2\sigma_i^2}}$$

2d Gaussian

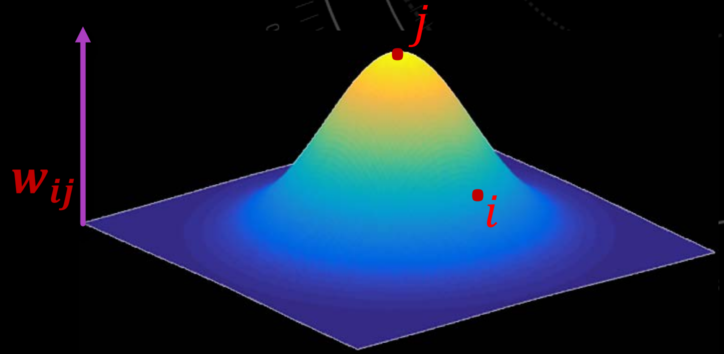

GAMMA TARGET CR PROBABILITY DENSITY

PoS (ICRC2023) 246

- CR event i weight equal to probability of originating at source j

$$w_{ij} = \frac{1}{2\pi\sigma_i^2} e^{-\frac{\xi_{ij}^2}{2\sigma_i^2}}$$

2d Gaussian

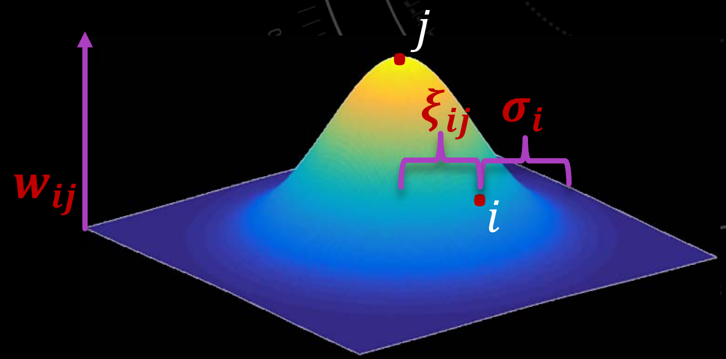

- ξ_{ij} - Angular distance between event i and source j
- σ_i - Pointing direction angular uncertainty
  - Function of zenith angle θ and m triggered SD

GAMMA TARGET CR PROBABILITY DENSITY

PoS (ICRC2023) 246

- CR event i weight equal to probability of originating at source j

$$w_{ij} = \frac{1}{2\pi\sigma_i^2} e^{-\frac{\xi_{ij}^2}{2\sigma_i^2}}$$

2d Gaussian

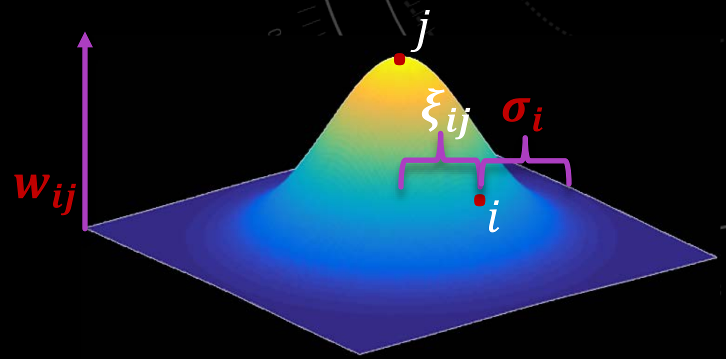

- ξ_{ij} - Angular distance between event i and source j
- σ_i - Pointing direction angular uncertainty
  - Function of zenith angle θ and m triggered SD

1500 meter array
E_{CR} > 1 EeV

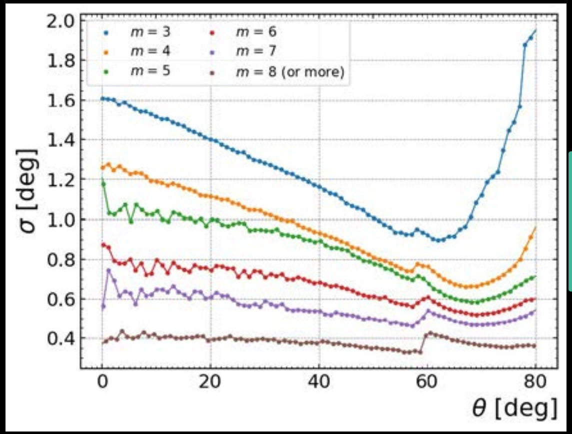

Pointing Direction Uncertainty

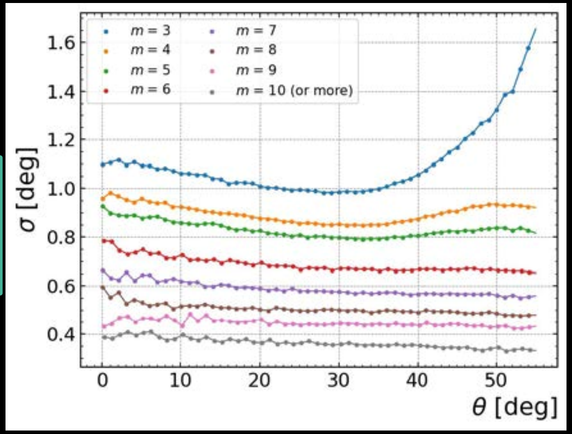

750 meter array
0.1 EeV < E_{CR} < 1 EeV

NEUTRON FLUX IDENTIFICATION

PoS (ICRC2023) 246

- All events considered possible source neutrons.
- Target j CR density:

$$\rho_j^{obs} = \sum_{i=1}^{N} w_i$$

NEUTRON FLUX IDENTIFICATION

PoS (ICRC2023) 246

- All events considered possible source neutrons.
- Target j CR density:

$$\rho_j^{obs} = \sum_{i=1}^{N} w_i$$

- Isotropic Monte Carlo simulations via shower observable scrambling:
  - Same N events as data.
  - Data sample trigger time t_i.
  - Sample zenith θ_i and associated σ_i.
  - Uniform azimuthal angle sampling ($0 \; to \; 2\pi$).
- p-val of ρ_j^{obs} via simulated event sets:

$$p_j = \frac{1}{N_{MC}} \sum_{k=1}^{N_{MC}} I\left(\rho_{kj}^{iso} > \rho_j^{obs}\right)$$

$$N_{MC} = 10,000$$

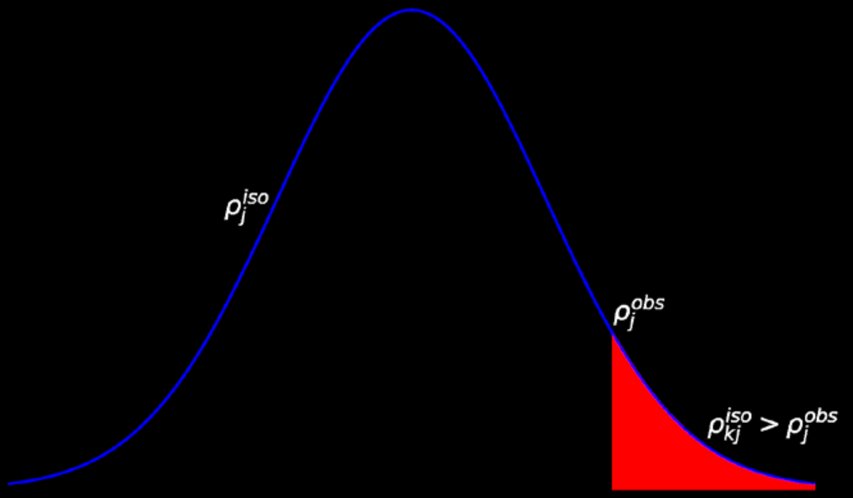

POSSIBLE SOURCES

PoS (ICRC2023) 246

- **12 Sources Classes Considered:**
  - **Same catalogs as** 1406.4038 (arxiv.org)

POSSIBLE SOURCES

PoS (ICRC2023) 246

- 12 Sources Classes Considered:
  - Same catalogs as 1406.4038 (arxiv.org)

High Energy Set (Dec. < 45°, $E_{CR} > 1$ EeV)

1. Millisecond Pulsars (msec PSRs): $\mathrm{N_{scrs}} = 283$
2. γ-ray Pulsars: 261
3. Low Mass X-ray Binaries (LMXB): 102
4. High Mass X-ray Binaries (HMXB): 60
5. γ TeV emitters - Pulsar Wind Nebulae (H.E.S.S. PWN): 28
6. γ TeV emitters – Other (H.E.S.S. other): 45
7. γ TeV emitters – Unidentified (H.E.S.S. UNID): 56
8. Microquasars: 15
9. Magnetars: 27
10. LHAASO PeVatrons (LHAASO): 9
11. Crab Nebula: 1
12. Galactic Center: 1

Low Energy Set (0.1 Eev < E_{CR} < 1 EeV) D < 1 kpc, Dec. < 20°,

1. msec PSRs: 25
2. γ-ray Pulsars: 113
4. HMXB: 8
5. H.E.S.S. PWN: 5
6. H.E.S.S. other: 11
9. Magnetars: 4

MOST SIGNIFICANT SOURCES

PoS (ICRC2023) 246

- **Sources Considered**
  - **12 source class sets:** 888 sources, Dec. up to 45° (E_{CR} > 1 EeV).
  - 166: D < 1 kpc and Dec. up to 20° (0.1 Eev < E_{CR} < 1 EeV).

~2.2σ

Most significant target from each target set ≥ 1 EeV

Class	R.A. [deg]	Dec. [deg]	p	p*
msec PSRs	286.2	2.1	0.0075	0.88
γ-ray PSRs	296.6	−54.1	5.0×10^{-5}	0.013
LMXB	237.00	−62.6	0.0069	0.51
HMXB	308.1	41.0	0.014	0.57
H.E.S.S. PWN	128.8	−45.6	0.0070	0.18
H.E.S.S. other	128.8	−45.2	0.022	0.63
H.E.S.S. UNID	305.0	40.8	0.0066	0.31
Microquasars	308.1	41.0	0.014	0.19
Magnetars	249.0	−47.6	0.15	0.99
LHAASO	292.3	17.8	0.024	0.20
Crab	83.6	22.0	0.71	…
Gal. Center	266.4	−29.0	0.86	…

Most Significant Source p-val

$$p^* = 1 - (1 - p)^N$$

(Šidák correction)

MOST SIGNIFICANT SOURCES

PoS (ICRC2023) 246

- **Sources Considered**
  - 12 source class sets: 888 sources, Dec. up to 45° (E_{CR} > 1 EeV).
  - 166: D < 1 kpc and Dec. up to 20° (0.1 Eev < E_{CR} < 1 EeV).

Most significant target from each target set $\geq$ 1 EeV				
Class	R.A. [deg]	Dec. [deg]	p	p*
msec PSRs	286.2	2.1	0.0075	0.88
γ-ray PSRs	296.6	−54.1	5.0×10^{-5}	0.013
LMXB	237.00	−62.6	0.0069	0.51
HMXB	308.1	41.0	0.014	0.57
H.E.S.S. PWN	128.8	−45.6	0.0070	0.18
H.E.S.S. other	128.8	−45.2	0.022	0.63
H.E.S.S. UNID	305.0	40.8	0.0066	0.31
Microquasars	308.1	41.0	0.014	0.19
Magnetars	249.0	−47.6	0.15	0.99
LHAASO	292.3	17.8	0.024	0.20
Crab	83.6	22.0	0.71	...
Gal. Center	266.4	−29.0	0.86	...

Same most significant H.E.S.S. PWN as 2014 result (p*-val = 0.56, 1406.4038)

Most Significant Source p-val

$$p^* = 1 - (1 - p)^N$$

(Šidák correction)

MOST SIGNIFICANT SOURCES

PoS (ICRC2023) 246

- **Sources Considered**
  - 12 source class sets: 888 sources, Dec. up to 45° (E_{CR} > 1 EeV).
  - 166: D < 1 kpc and Dec. up to 20° (0.1 Eev < E_{CR} < 1 EeV).

~2.2σ (γ-ray PSRs)

Most significant target from each target set $\geq$ 1 EeV

Class	R.A. [deg]	Dec. [deg]	p	p^*
msec PSRs	286.2	2.1	0.0075	0.88
γ-ray PSRs	296.6	−54.1	5.0×10^{-5}	0.013
LMXB	237.00	−62.6	0.0069	0.51
HMXB	308.1	41.0	0.014	0.57
H.E.S.S. PWN	128.8	−45.6	0.0070	0.18
H.E.S.S. other	128.8	−45.2	0.022	0.63
H.E.S.S. UNID	305.0	40.8	0.0066	0.31
Microquasars	308.1	41.0	0.014	0.19
Magnetars	249.0	−47.6	0.15	0.99
LHAASO	292.3	17.8	0.024	0.20
Crab	83.6	22.0	0.71	…
Gal. Center	266.4	−29.0	0.86	…

Most significant target from each target set $\geq$ 0.1 EeV

Class	R.A. [deg]	Dec. [deg]	p	p^*
msec PSRs	140.5	−52.0	0.043	0.66
γ-ray PSRs	288.4	10.3	0.0056	0.47
HMXB	116.9	−53.3	0.0092	0.071
H.E.S.S. PWN	277.9	−9.9	0.12	0.48
H.E.S.S. other	288.2	10.2	0.0033	0.036
Magnetars	274.7	−16.0	0.13	0.44

Most Significant Source p-val

$$p^* = 1 - (1 - p)^N$$

(Šidák correction)

NEUTRON SOURCE UPPER LIMITS

PoS (ICRC2023) 246

Upper limit neutron number n_j^{UL} for a target source j is $max(n)$ with fractions:

$$f_n < (1 - CL_{95\%}) f_0$$

- $f_0 = \frac{1}{N_{MC}} \sum_{k=1}^{N_{MC}} I\left(\rho_{kj}^{iso} < \rho_j^{obs}\right)$ **(MC < density than obs.)**
- $f_n = \frac{1}{N_{MC}} \sum_{k=1}^{N_{MC}} I\left(\rho_{kj}^{iso+n} < \rho_j^{obs}\right)$ **(MC + n events < density than obs.)**

NEUTRON SOURCE UPPER LIMITS

PoS (ICRC2023) 246

Flux Upper Limit:

$$\Phi_j^{UL} = \frac{n_j^{UL}}{\omega_j^{dir}}$$

Upper limit neutron number n_j^{UL} for a target source j is $max(n)$ with fractions:

$$f_n < (1 - CL_{95\%}) f_0$$

- $f_0 = \frac{1}{N_{MC}} \sum_{k=1}^{N_{MC}} I\left(\rho_{kj}^{iso} < \rho_j^{obs}\right)$ (MC < density than obs.)
- $f_n = \frac{1}{N_{MC}} \sum_{k=1}^{N_{MC}} I\left(\rho_{kj}^{iso+n} < \rho_j^{obs}\right)$ (MC + n events < density than obs.)

Directional Exposure

$$\omega_j^{dir} = \frac{\langle \rho_{kj}^{iso} \rangle}{I_{CR}} = \frac{\rho_j^{exp}}{I_{CR}}$$

I_{CR}: Intensity (integrated flux)

NEUTRON SOURCE UPPER LIMITS

PoS (ICRC2023) 246

Flux Upper Limit:

$$\Phi_j^{UL} = \frac{n_j^{UL}}{\omega_j^{dir}}$$

Upper limit neutron number n_j^{UL} for a target source j is $max(n)$ with fractions:

$$f_n < (1 - CL_{95\%}) f_0$$

- $f_0 = \frac{1}{N_{MC}} \sum_{k=1}^{N_{MC}} I(\rho_{kj}^{iso} < \rho_j^{obs})$ (MC < density than obs.)
- $f_n = \frac{1}{N_{MC}} \sum_{k=1}^{N_{MC}} I(\rho_{kj}^{iso+n} < \rho_j^{obs})$ (MC + n events < density than obs.)

Directional Exposure

$$\omega_j^{dir} = \frac{\langle \rho_{kj}^{iso} \rangle}{I_{CR}} = \frac{\rho_j^{exp}}{I_{CR}}$$

I_{CR}: Intensity (integrated flux)

Most significant target from each target set ≥ 1 EeV

Class	R.A. [deg]	Dec. [deg]	Flux U.L. [km^{-2} yr^{-1}]	E-Flux U.L. [eV cm^{-2} s^{-1}]
msec PSRs	286.2	2.1	0.026	0.19
γ-ray PSRs	296.6	−54.1	0.023	0.17
LMXB	237.0	−62.6	0.017	0.12
HMXB	308.1	41.0	0.13	0.97
H.E.S.S. PWN	128.8	−45.6	0.016	0.12
H.E.S.S. other	128.8	−45.2	0.014	0.11
H.E.S.S. UNID	305.0	40.8	0.15	1.1
Microquasars	308.1	41.0	0.13	0.95
Magnetars	249.0	−47.6	0.011	0.079
LHAASO	292.3	17.8	0.038	0.28
Crab	83.6	22.0	0.020	0.15
Gal. Center	266.4	−29.0	0.0053	0.039

Down from 0.018

Assuming an E^{-2} spectrum

Most significant target from each target set ≥ 0.1 EeV

Class	R.A. [deg]	Dec. [deg]	Flux U.L. [km^{-2} yr^{-1}]	E-Flux U.L. [eV cm^{-2} s^{-1}]
msec PSRs	140.5	−52.0	1.7	12.5
γ-ray PSRs	288.4	10.3	5.3	38.9
HMXB	116.9	−53.3	2.1	15.1
H.E.S.S. PWN	277.9	−9.9	1.8	13.4
H.E.S.S. other	288.2	10.2	5.5	40.2
Magnetars	274.7	−16.0	1.6	11.8

SOURCE CLASS SIGNIFICANCE

PoS (ICRC2023) 246

- **Source class combined p-value:** prob. of multiplied N uniformly distributed numbers 0 < n < 1

$$p(\Pi < \Pi_0) = \Pi_0 \sum_{k=0}^{N-1} \frac{(-\ln \Pi_0)^k}{k!} = 1 - Poisson(N, \ln \Pi_0)$$

$$\Pi_0 = \prod_{j=1}^{N} p_j$$

Multiply source p-values

SOURCE CLASS SIGNIFICANCE

PoS (ICRC2023) 246

- **Source class combined p-value:** prob. of multiplied N uniformly distributed numbers 0 < n < 1

$$p(\Pi < \Pi_0) = \Pi_0 \sum_{k=0}^{N-1} \frac{(-\ln \Pi_0)^k}{k!} = 1 - Poisson(N, \ln \Pi_0)$$

$$\Pi_0 = \prod_{j=1}^{N} p_j$$

Multiply source p-values

Combined P-value $\geq$ 1 EeV			
Class	No.	P-value	P-value (weighted)
msec PSRs	283	0.90	0.50
γ-ray PSRs	261	0.16	0.020
LMXB	102	0.62	0.25
HMXB	60	0.49	0.34
H.E.S.S. PWN	28	0.24	0.0052
H.E.S.S. other	45	0.52	0.22
H.E.S.S. UNID	56	0.61	0.75
Microquasars	15	0.39	0.81
Magnetars	27	0.99	0.98
LHAASO	9	0.22	0.42
Crab	1	0.71	...
Gal. Center	1	0.86	...

~2.6σ

1,500 m array data set

Combined P-value $\geq$ 0.1 EeV			
Class	No.	P-value	P-value (weighted)
msec PSRs	25	0.82	0.58
γ-ray PSRs	113	0.53	0.93
HMXB	8	0.33	0.23
H.E.S.S. PWN	5	0.43	0.83
H.E.S.S. other	11	0.074	0.58
Magnetars	4	0.31	0.14

750 m array data set

$$\Pi_w = \prod_{j=1}^{N} p_j^{w_j}$$

Source weighted p-vals by EM-flux, exposure, and neutron decay attenuation factor

NEUTRON SUMMARY

- No significant evidence of neutron fluxes from candidate sources.
- Energy flux upper limits below TeV gamma-ray energy fluxes.
  - Neutron energy flux should exceed gamma-ray flux (more efficient production with E^-2 Fermi Acceleration).
- E_{CR} > 1 EeV all extragalactic? Transient sources? Misaligned sources?

NEUTRON SUMMARY

- No significant evidence of neutron fluxes from candidate sources.
- Energy flux upper limits below TeV gamma-ray energy fluxes.
  - Neutron energy flux should exceed gamma-ray flux
    (more efficient production with E^-2 Fermi Acceleration).
- E_{CR} > 1 EeV all extragalactic? Transient sources? Misaligned sources?

See also Federico Maria Mariani's ICNFP2024 talk "Anisotropy searches of cosmic rays at the highest energy with the Pierre Auger Observatory"

SUMMARY

- Lack of detections does not mean great science cannot be done! E.g.
  - Limits on stellar object mergers proportion of energy in neutrinos/photons.
  - Some dark matter models excluded from decay into large flux of neutrinos/photons.
  - Further evidence of extragalactic UHECR.
  - Exclusions of UHECR compositions and source redshift evolution models.

See David Schmidt's ICNFP2024 talk
"AugerPrime: Expectations and first results"

- Future possible first detections and significant improvements in point source upper limits for neutrinos/photons/neutrons.